

**FIRST LIGHT
ADVANCED SCHOOL 2019**

GALAXY FORMATION

**Patricia B. Tissera
Universidad Andrés Bello
Chile**



**Universidad
Andrés Bello**

Lecture.I

Galaxy formation: From the high-z to the Local Universe

Lecture.II

Galaxy formation: models and simulations

- Basic concepts
- Main ingredients
- Disc-dominated and Bulge-dominated galaxies

Lecture.II

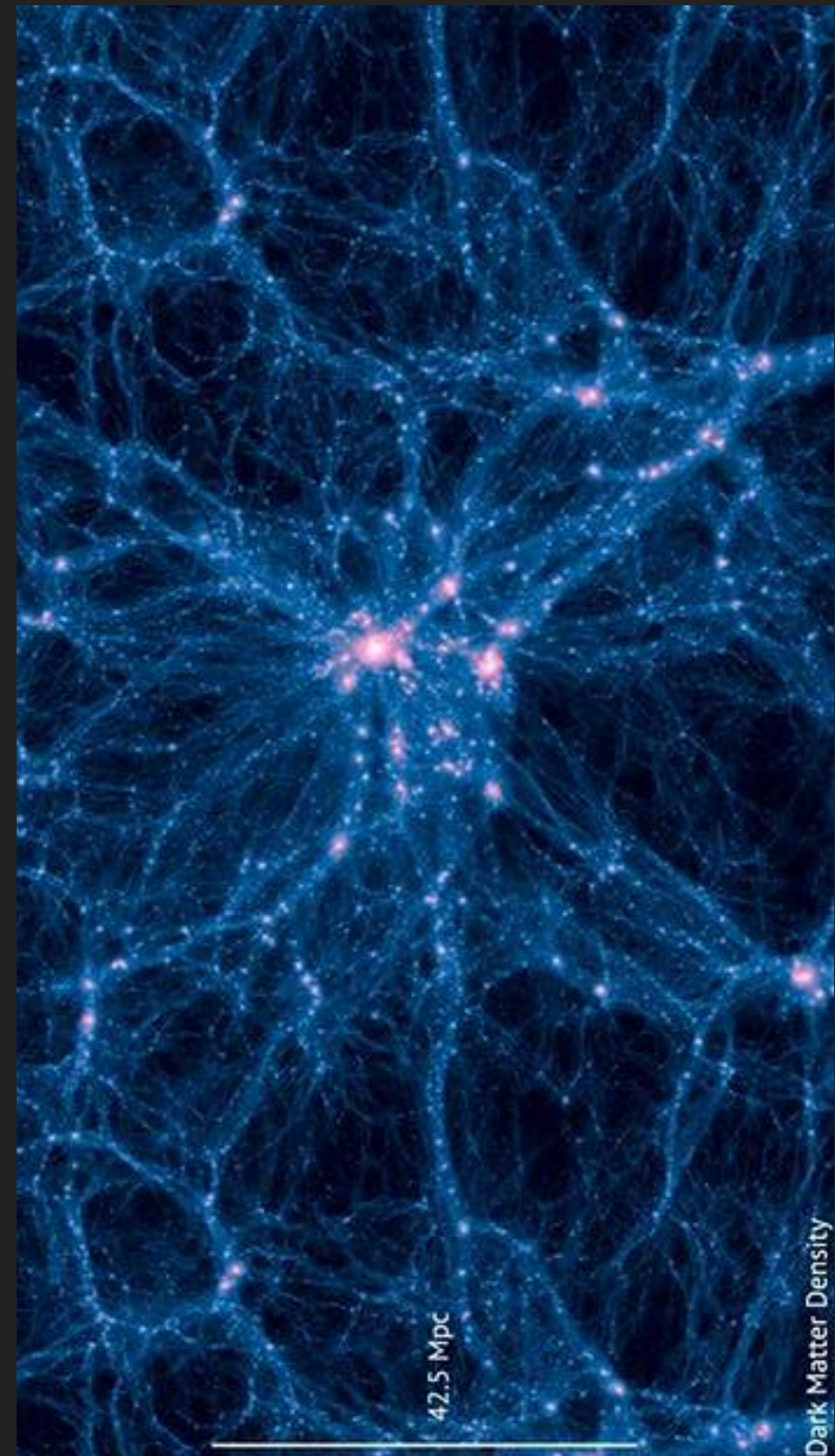
Galaxy formation: chemical evolution

first galaxies

$z \sim 0$



- + Initial conditions : Λ CDM
- + Gravity: large and intermediate scale evolution
- + Gas cooling
- + Star formation
- + Stellar evolution: energy and chemical feedback
- + AGN feedback
- + others: Cosmic rays, Magnetic fields
- + etc

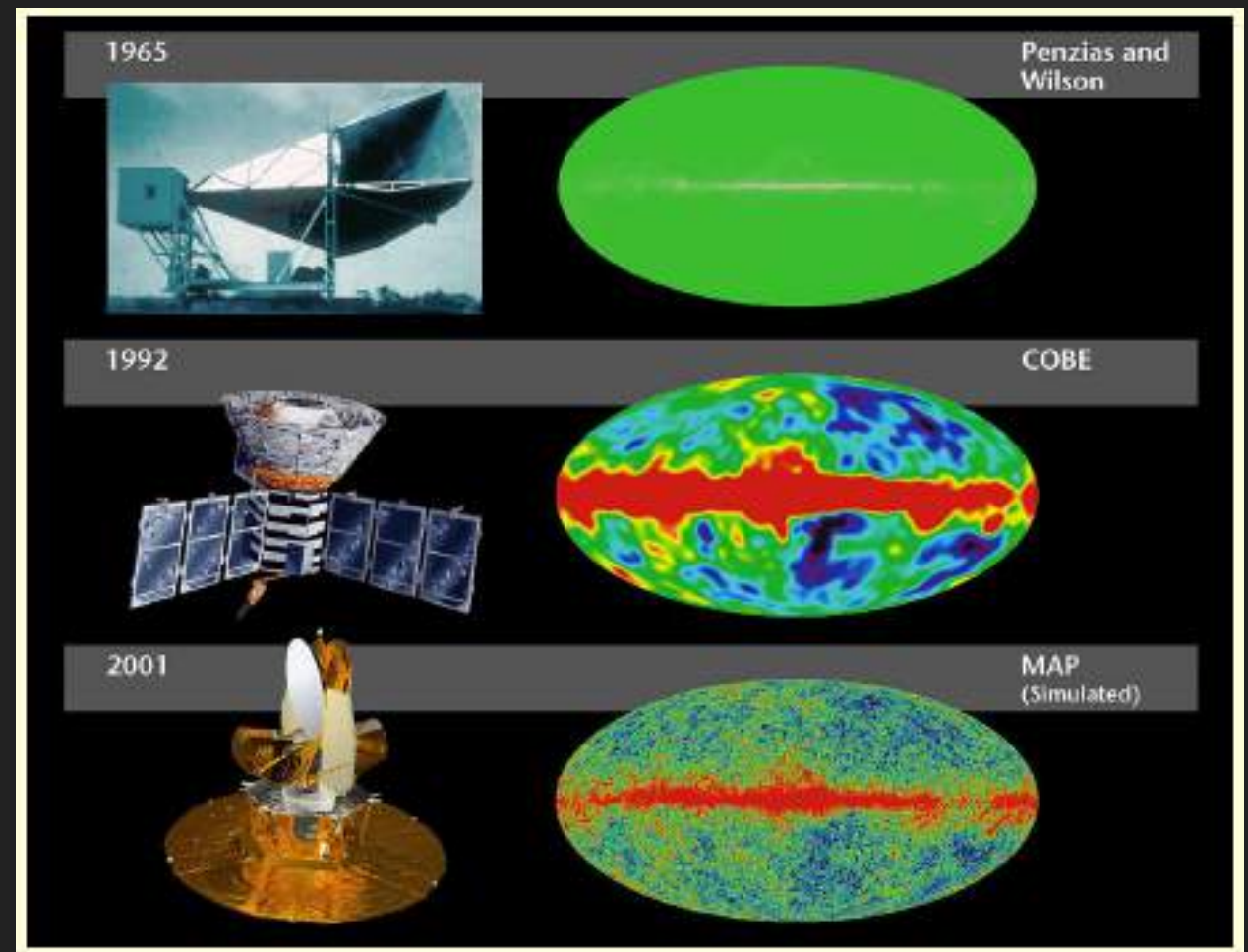


Gravitational instability scenario assumes the early universe to be almost perfectly smooth, with the exception of tiny density deviations with respect to the background density.

These small perturbations are accompanying by small velocity perturbation to the general Hubble expansion.

From the CMB observations:

$$\Delta T \sim 10^{-5} \text{ K}$$



The CMB research history:

- 1) The discovery of the CMB by Penzias & Wilson in 1965.
- 2) The COBE satellite, first discovery of the primordial fluctuations in 1992.
- 3) WMAP (2003) detailed temperature perturbations 'fix' the universe's parameters.

$$\delta\rho/\rho \ll 1$$

$$\frac{d^2\delta(\mathbf{x}, t)}{dt^2} + 2\frac{\dot{a}(t)}{a(t)}\frac{d\delta(\mathbf{x}, t)}{dt} = \frac{c_s^2}{a(t)^2}\nabla^2\delta(\mathbf{x}, t) + 4\pi G\bar{\rho}(t)\delta(\mathbf{x}, t),$$

$$\frac{d^2\delta_{\mathbf{k}}}{dt^2} + 2H(t)\frac{d\delta_{\mathbf{k}}}{dt} = \delta_{\mathbf{k}}\left(4\pi G\bar{\rho}(t) - \frac{k^2 c_s^2}{a(t)^2}\right).$$

$$\delta\rho/\rho \sim 1$$

$$\lambda_J = \frac{2\pi a(t)}{k_J} = c_s \left(\frac{\pi}{G\bar{\rho}}\right)^{1/2}$$

$$M_J = \frac{4\pi}{3}\rho \left(\frac{\lambda_J}{2}\right)^3.$$

Jeans scale: pressure gradients balance gravity

Jeans Mass: the minimum mass that can collapse

For $\lambda \gtrsim \lambda_J$, the time for pressure response is larger than the perturbation growth time.

If the fluctuations are $\delta\rho/\rho \ll 1$ \rightarrow

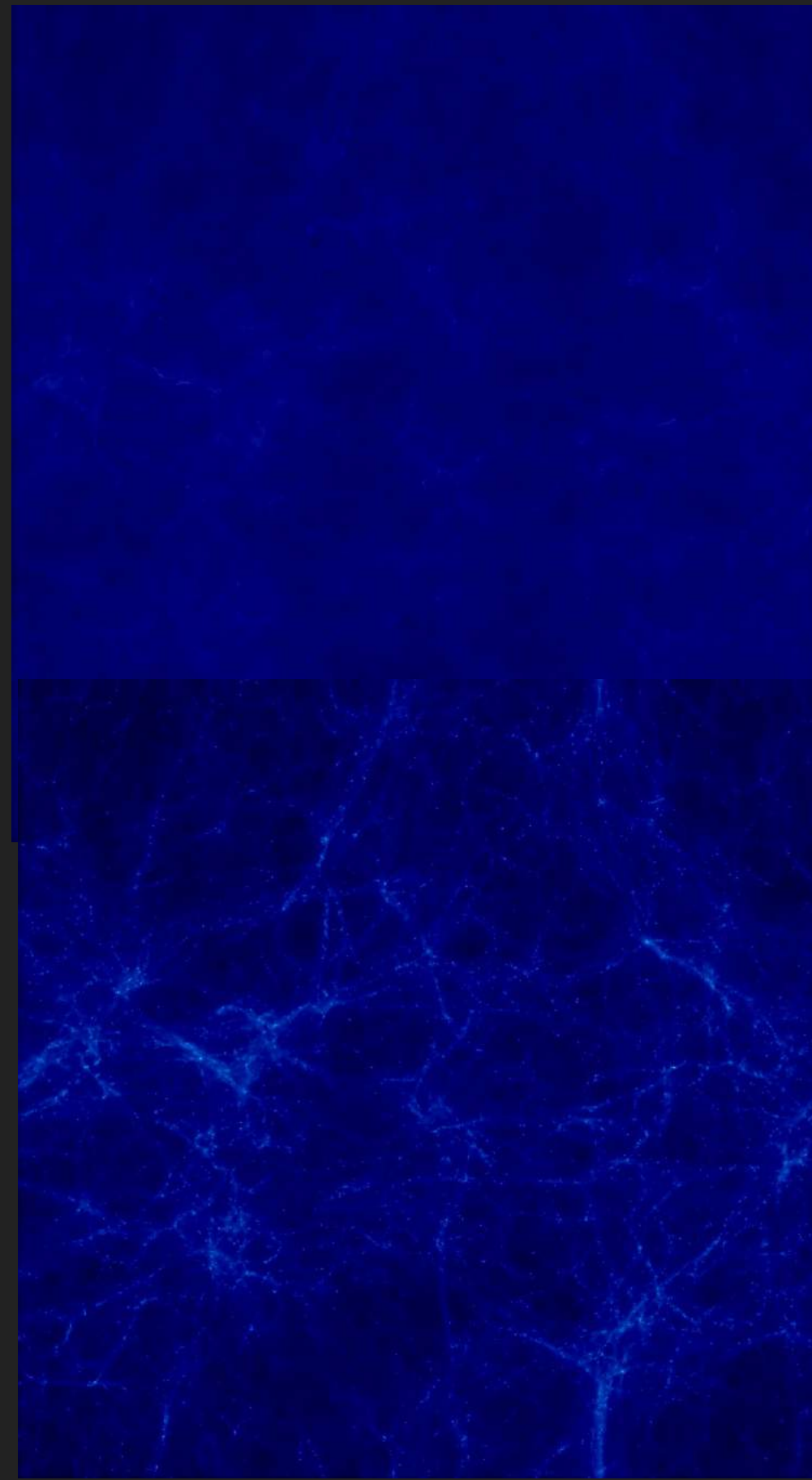
they grow via gravity and can be described by linear perturbation theory.

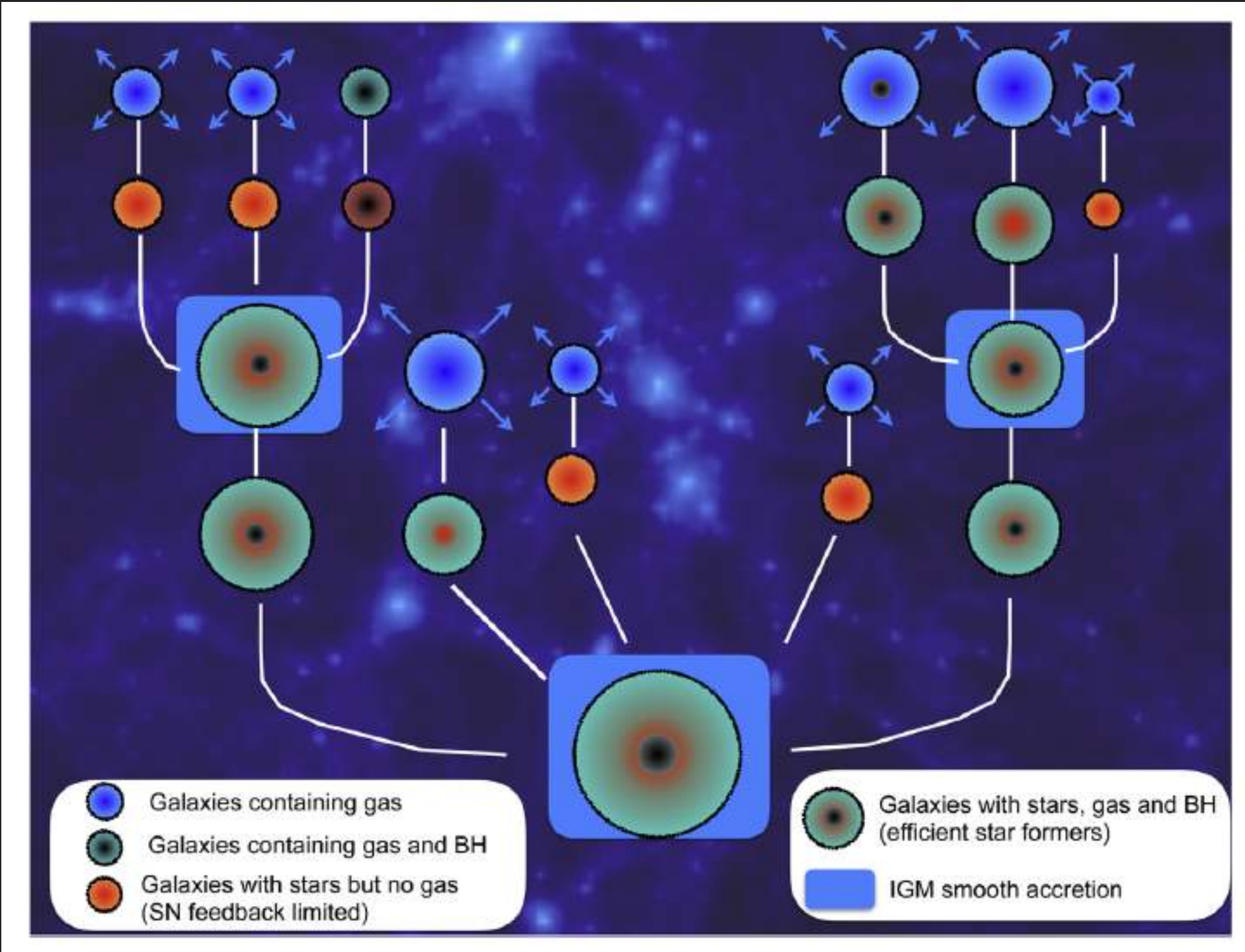
When they grow so that $\delta\rho/\rho \sim 1$ \rightarrow

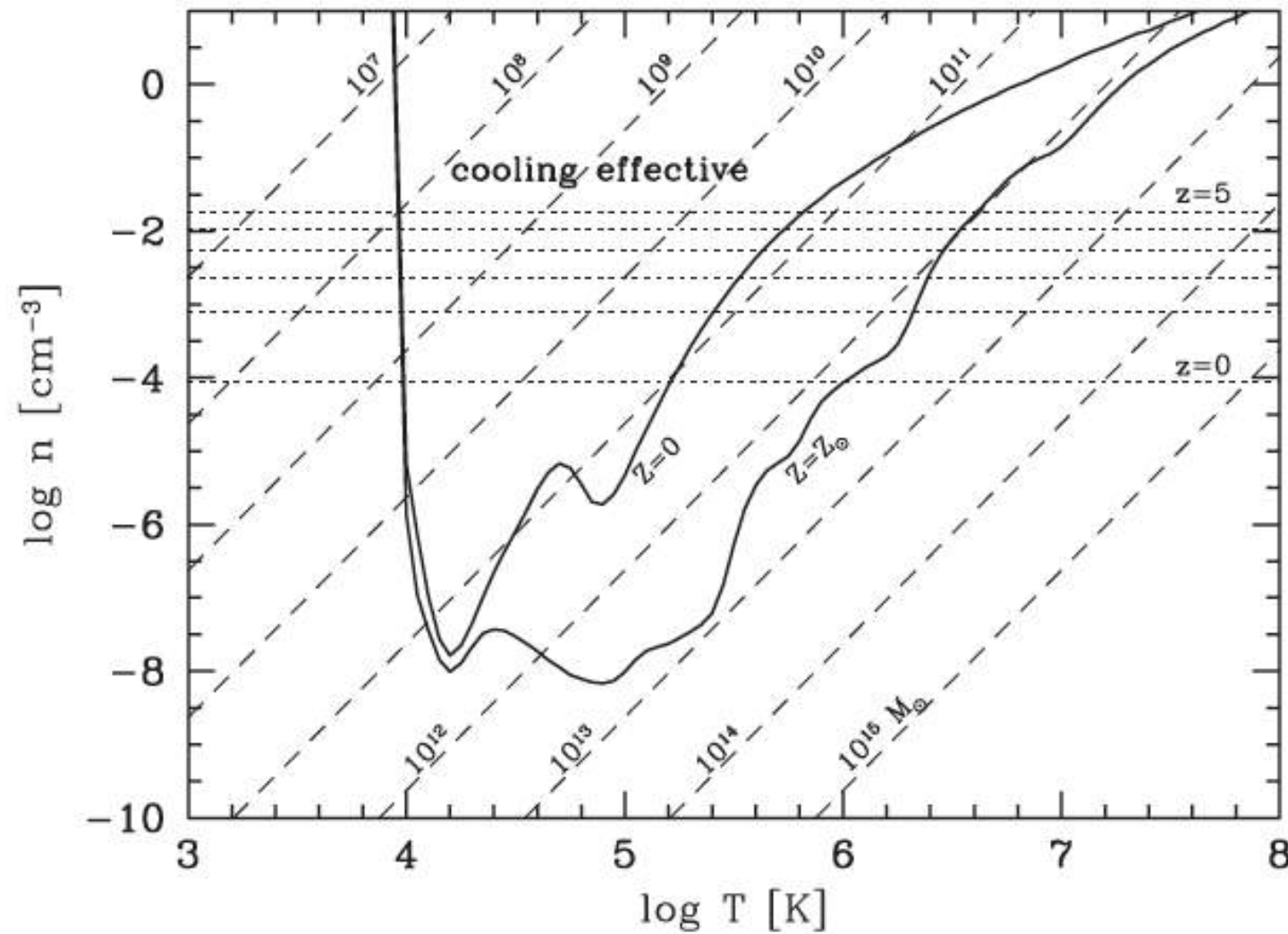
They are able to separate from the global expansion and collapse to form a bounded system.

At the turnaround radius, fluctuations reach its maximum radius and collapse, entering the non-linear regime.

Finally, the system will reach virialization.





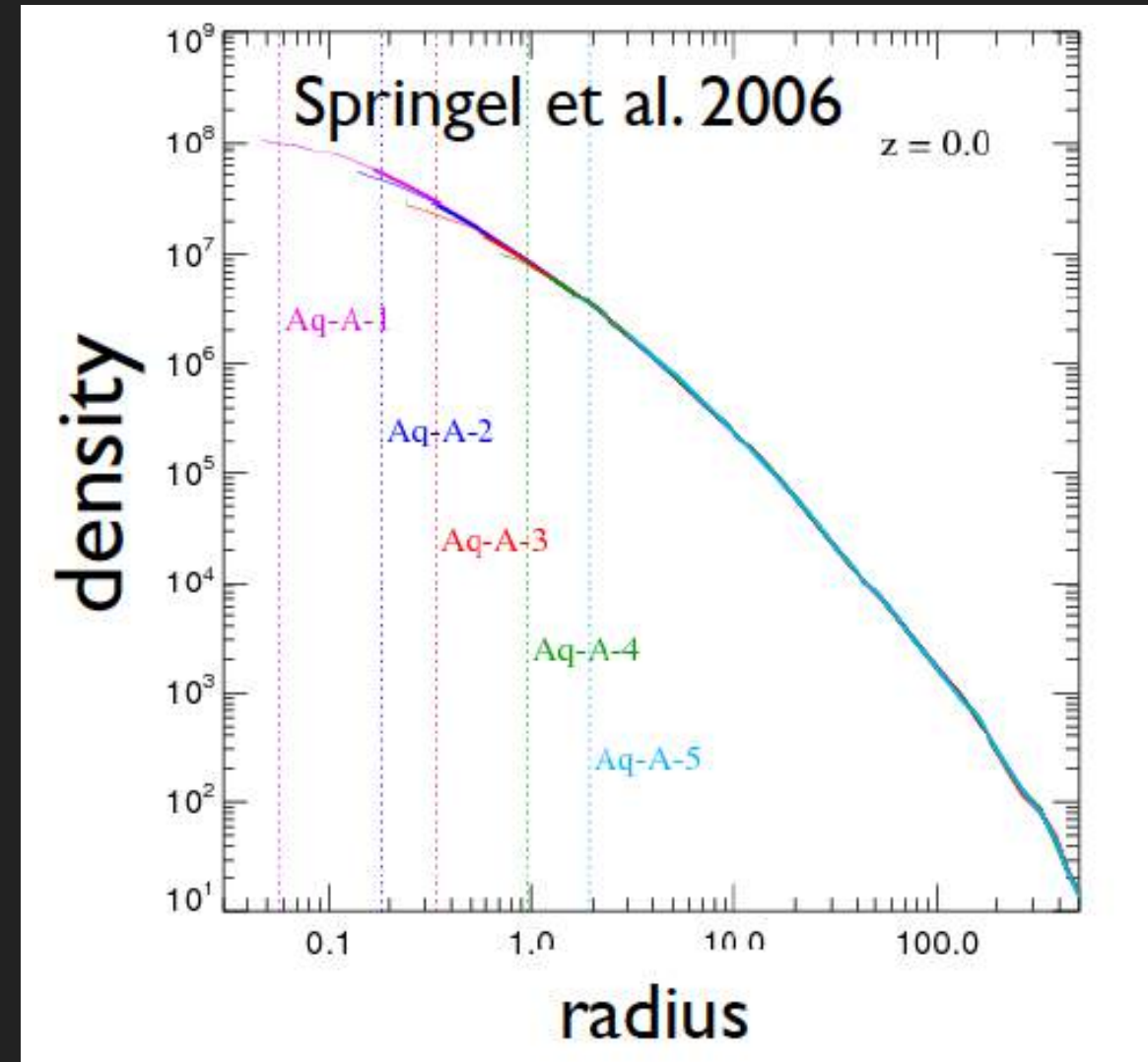
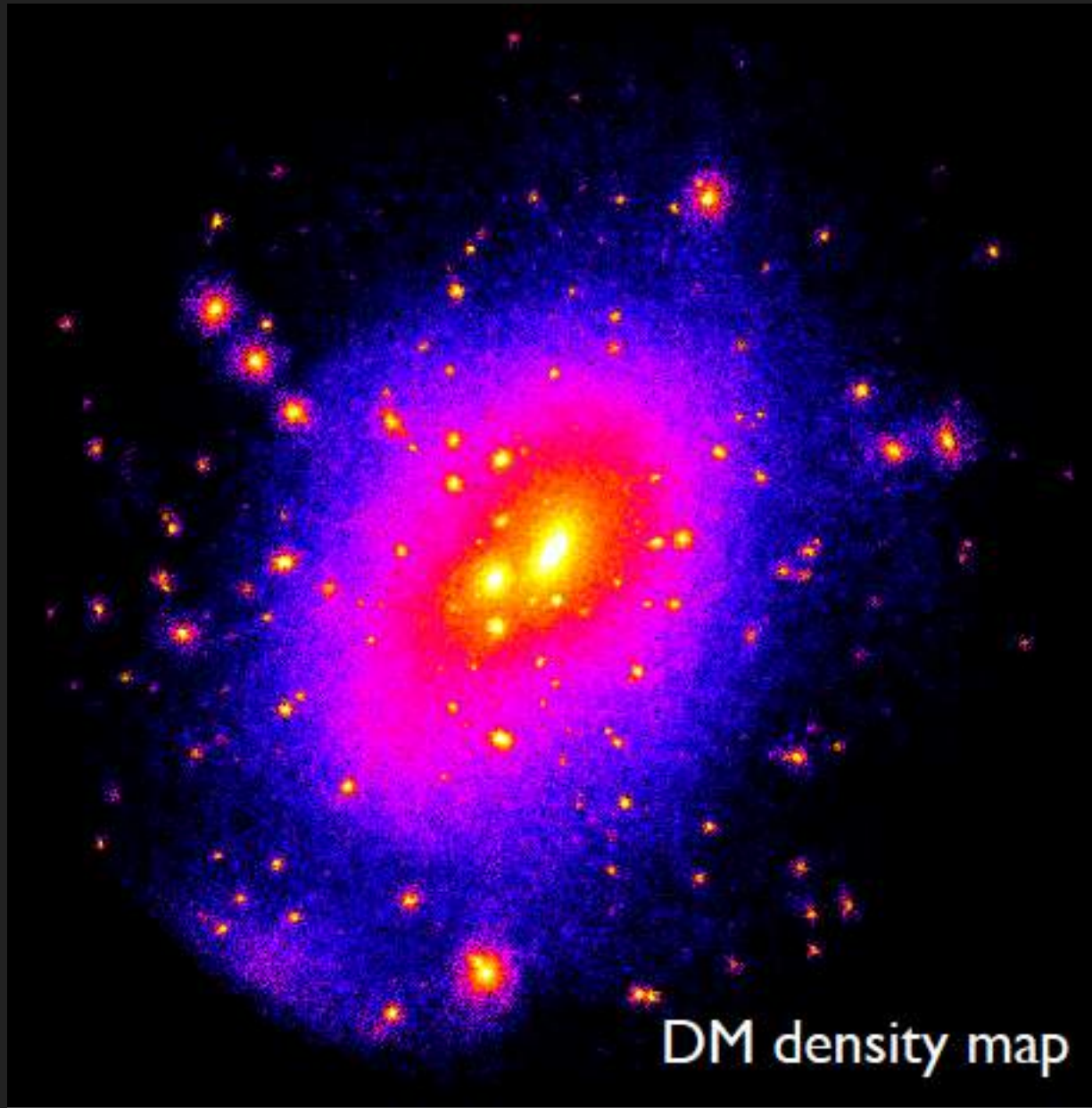


virialised haloes

Fig. 8.6. Cooling diagram showing the locus of $t_{\text{cool}} = t_{\text{ff}}$ in the n - T plane. The upper and lower curves correspond to gas with zero and solar metallicity, respectively. The tilted dashed lines are lines of constant gas mass (in M_{\odot}), while the horizontal dotted lines show the gas densities expected for virialised haloes ($\delta = 200$) at different redshifts. All calculations assume $f_{\text{gas}} = 0.15$, $\Omega_{m,0} = 0.3$, and $h = 0.7$. Cooling is effective for clouds with n and T above the locus.

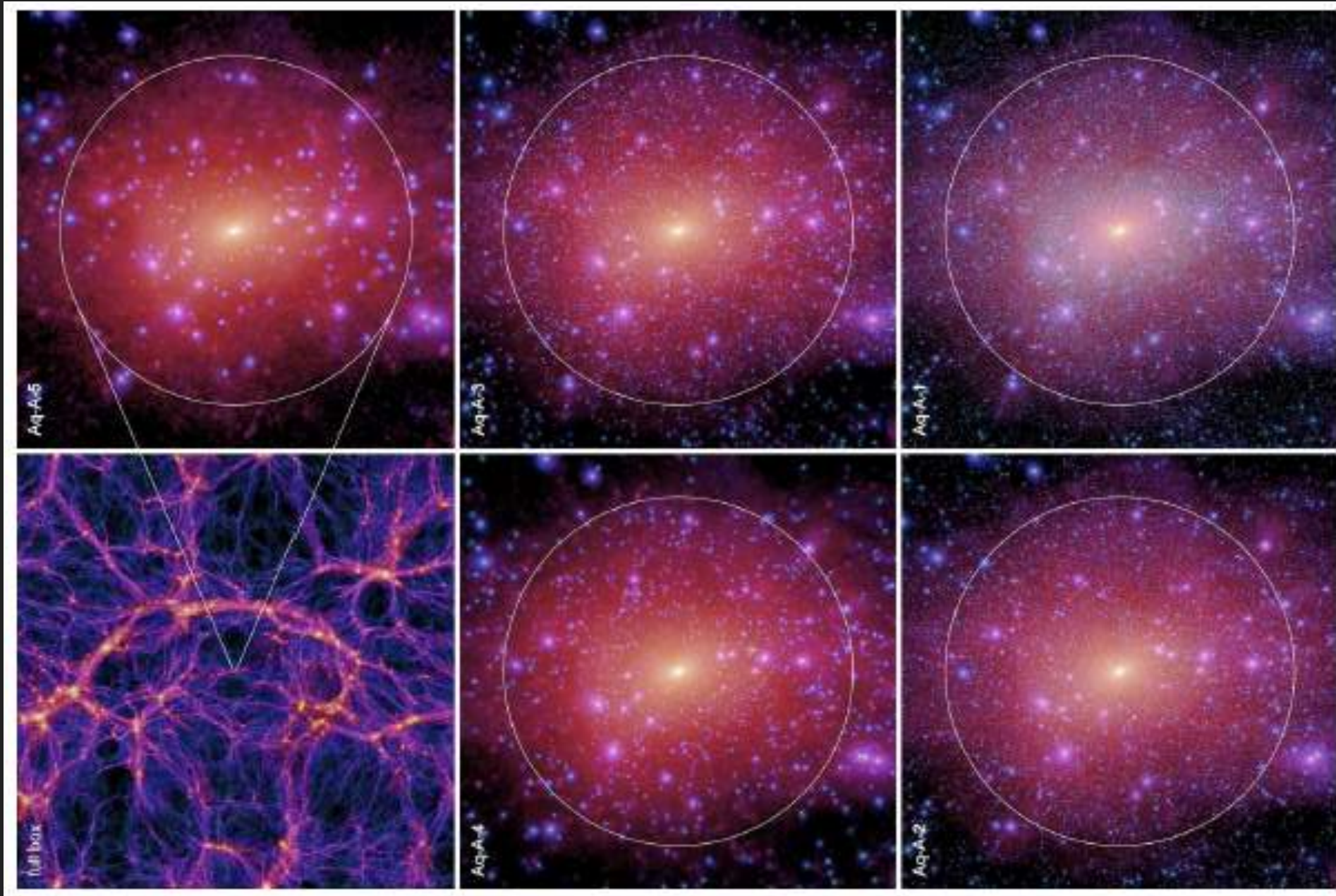
$$t_{\text{ff}} = \sqrt{\frac{3\pi}{32G\rho}} = \sqrt{\frac{3\pi f_{\text{gas}}}{32Gn\mu m_p}} \approx 2.1 \times 10^9 f_{\text{gas}}^{1/2} n_{-3}^{-1/2} \text{ yr},$$

$$t_{\text{cool}} \equiv \frac{\rho \mathcal{E}}{\mathcal{C}} = \frac{3nk_{\text{B}}T}{2n_{\text{H}}^2 \Lambda(T)} \approx 3.3 \times 10^9 \frac{T_6}{n_{-3} \Lambda_{-23}(T)} \text{ yr},$$



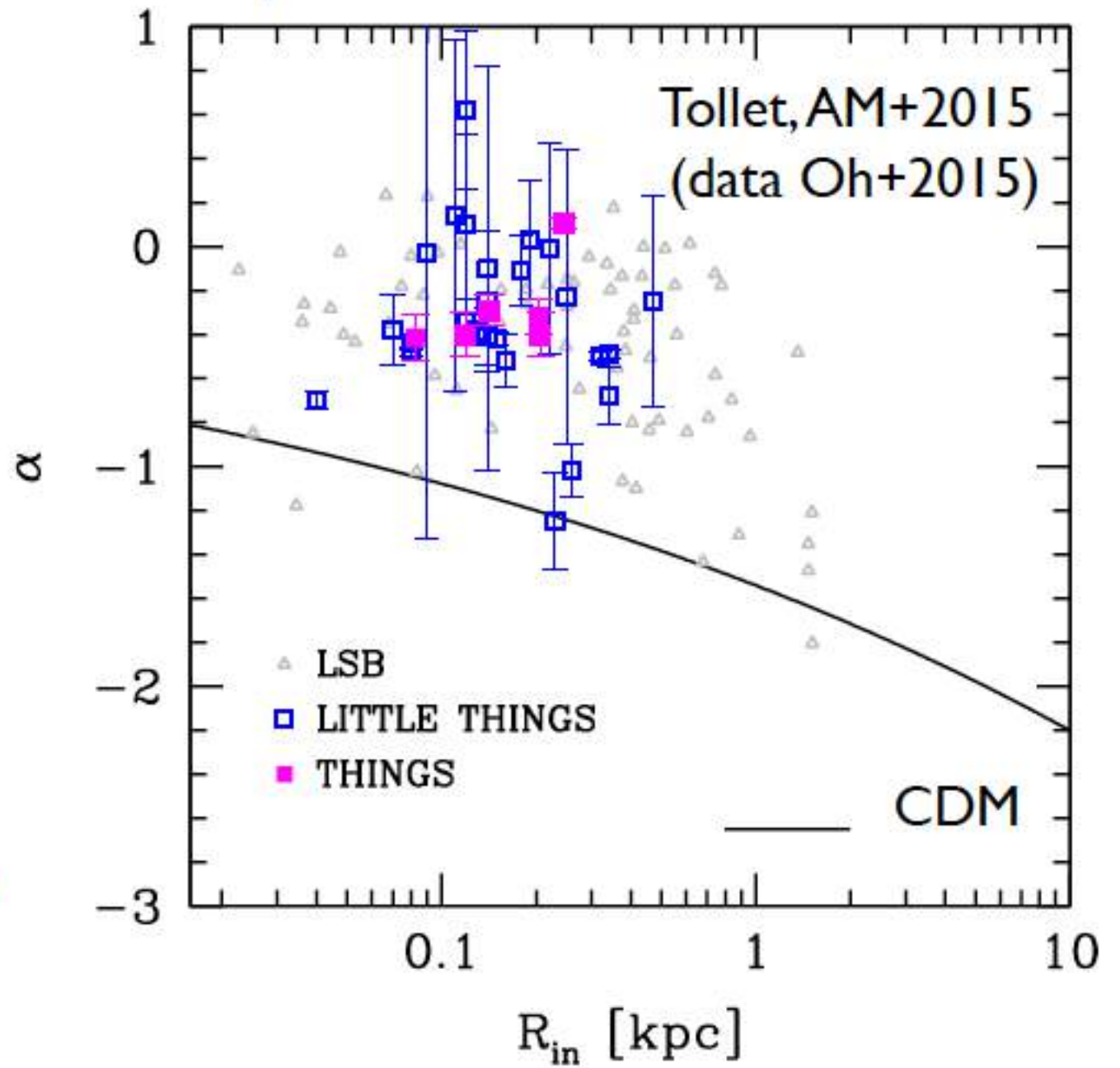
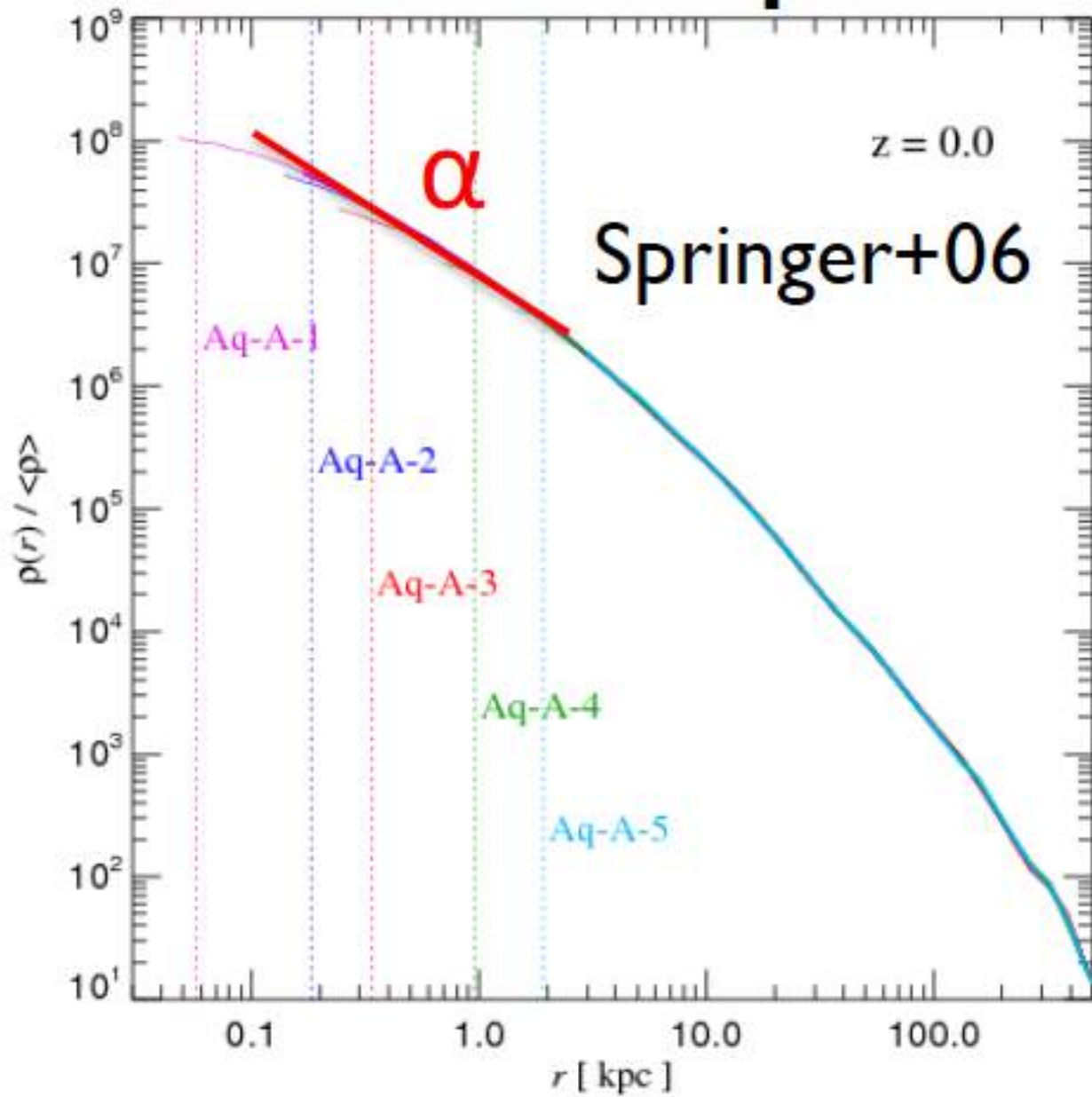
Dark matter evolution is well described numerically by N-body codes

Dark matter profiles are self-similar



Name	m_p [M_\odot]	ϵ [pc]	N_{hr}	N_{lr}	M_{200} [M_\odot]	r_{200} [kpc]	M_{50} [M_\odot]	r_{50} [kpc]	N_{50}
Aq-A-1	1.712×10^3	20.5	4,252,607,000	144,979,154	1.839×10^{12}	245.76	2.523×10^{12}	433.48	1,473,568,512
Aq-A-2	1.370×10^4	65.8	531,570,000	75,296,170	1.842×10^{12}	245.88	2.524×10^{12}	433.52	184,243,536
Aq-A-3	4.911×10^4	120.5	148,285,000	20,035,279	1.836×10^{12}	245.64	2.524×10^{12}	433.50	51,391,468
Aq-A-4	3.929×10^5	342.5	18,535,972	634,793	1.838×10^{12}	245.70	2.524×10^{12}	433.52	6,424,399
Aq-A-5	3.143×10^6	684.9	2,316,893	634,793	1.853×10^{12}	246.37	2.541×10^{12}	434.50	808,479

Cusp vs. core problem



The governing equations of an *ideal* gas can also be written in **Lagrangian form**

BASIC HYDRODYNAMICAL EQUATIONS

Euler equation:
$$\frac{d\mathbf{v}}{dt} = -\frac{\nabla P}{\rho} - \nabla\Phi$$

Continuity equation:
$$\frac{d\rho}{dt} + \rho\nabla \cdot \mathbf{v} = 0$$

First law of thermodynamics:
$$\frac{du}{dt} = -\frac{P}{\rho}\nabla \cdot \mathbf{v} - \frac{\Lambda(u, \rho)}{\rho}$$

Equation of state of an ideal monoatomic gas:
$$P = (\gamma - 1)\rho u, \quad \gamma = 5/3$$

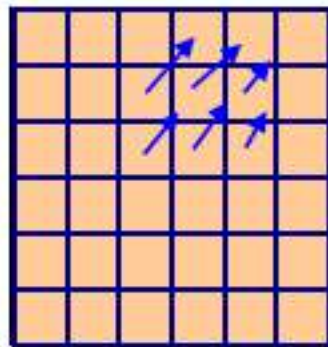
What is smoothed particle hydrodynamics?

DIFFERENT METHODS TO DISCRETIZE A FLUID

Eulerian

discretize space

representation on a mesh
(volume elements)



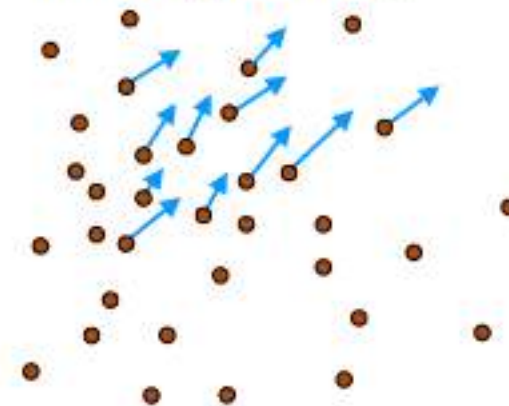
principle advantage:

high accuracy (shock capturing),
low numerical viscosity

Lagrangian

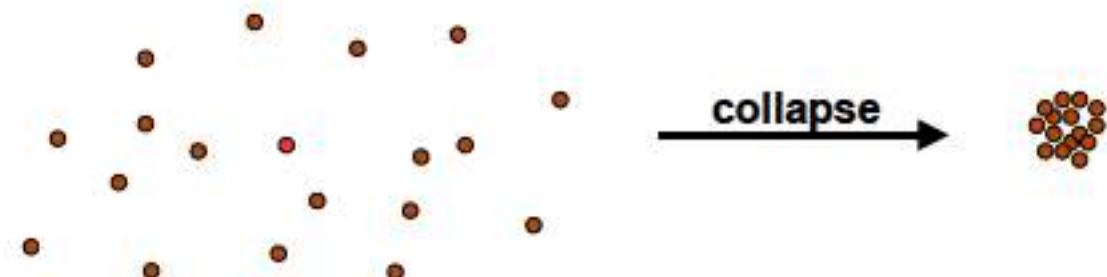
discretize mass

representation by fluid
elements (particles)



principle advantage:

resolutions adjusts
automatically to the flow



Kernel interpolation is used in smoothed particle hydrodynamics to build continuous fluid quantities from discrete tracer particles

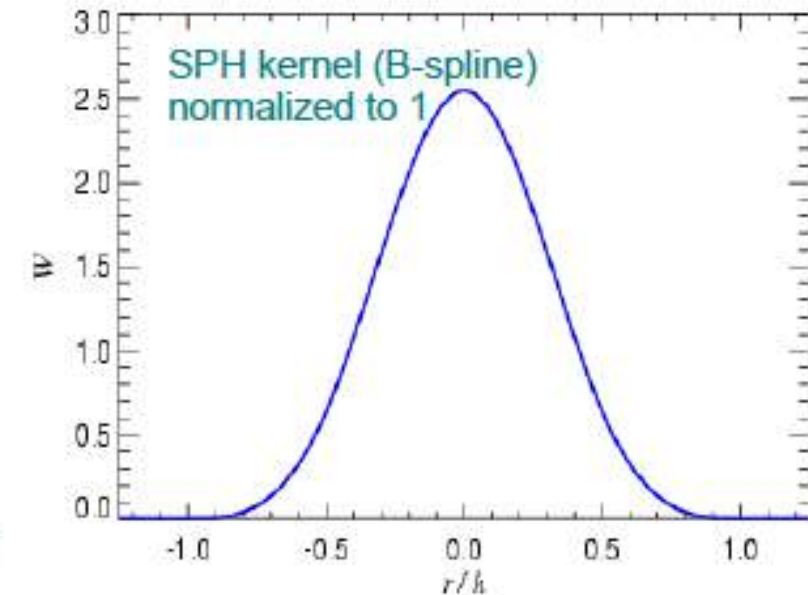
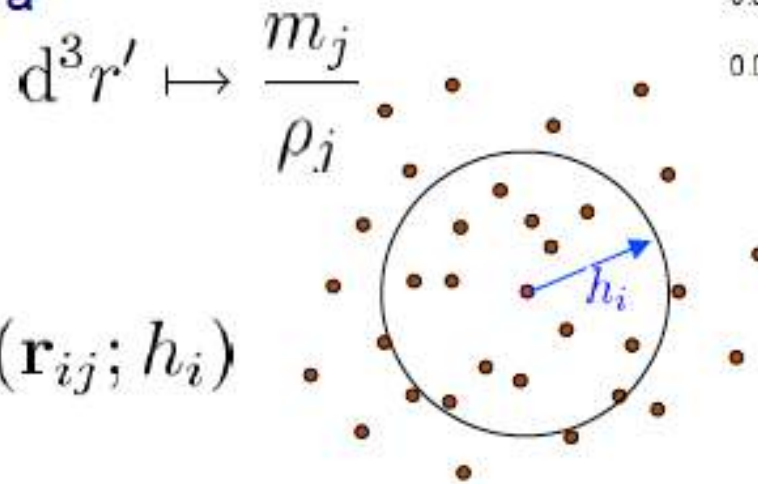
DENSITY ESTIMATION IN SPH BY MEANS OF ADAPTIVE KERNEL ESTIMATION

Kernel interpolant of an arbitrary function:

$$\langle A(\mathbf{r}) \rangle = \int W(\mathbf{r} - \mathbf{r}', h) A(\mathbf{r}') d^3r'$$

If the function is only known at a set of discrete points, we approximate the integral as a sum, using the replacement:

$$\langle A_i \rangle = \sum_{j=1}^N \frac{m_j}{\rho_j} A_j W(\mathbf{r}_{ij}; h_i)$$



This leads to the SPH density estimate, for $A_i = \rho_i$

$$\rho_i = \sum_{j=1}^N m_j W(|\mathbf{r}_{ij}|, h_i)$$

→ This can be differentiated !

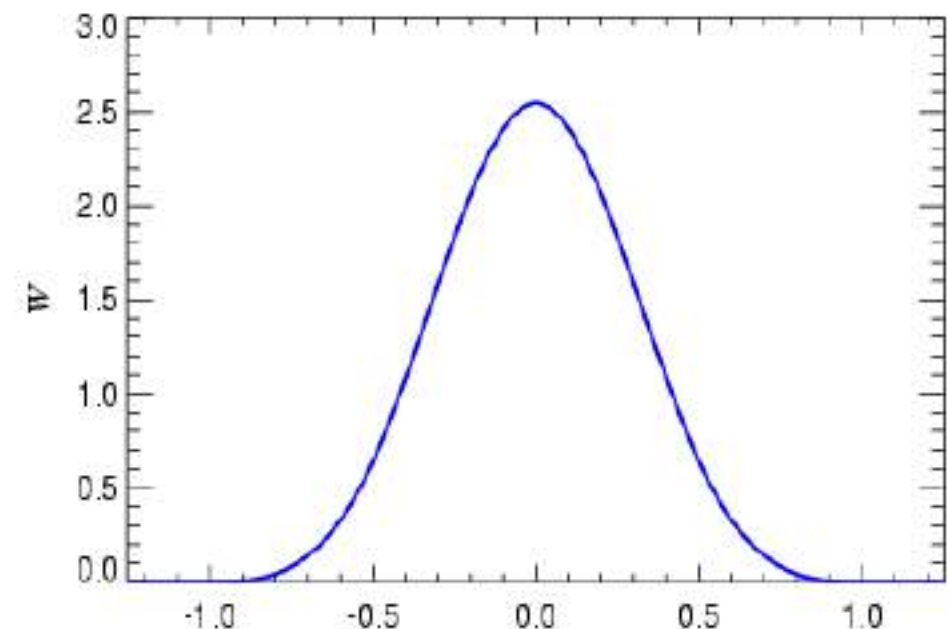
Good kernel shapes need to fulfill a number of constraints

CONDITIONS ON KERNELS

- ▶ Must be normalized to unity
- ▶ Compact support (otherwise N^2 bottleneck)
- ▶ High order of interpolation
- ▶ Spherical symmetry (for angular momentum conservation)

Nowadays, almost exclusively the cubic spline is used:

$$W(u) = \frac{8}{\pi} \begin{cases} 1 - 6u^2 + 6u^3, & 0 \leq u \leq \frac{1}{2}, \\ 2(1 - u)^3, & \frac{1}{2} < u \leq 1, \\ 0, & u > 1. \end{cases}$$



Smoothed particle hydrodynamics is governed by a set of ordinary differential equations

BASIC EQUATIONS OF SMOOTHED PARTICLE HYDRODYNAMICS

Each particle carries either the energy or the entropy per unit mass as independent variable

Density estimate $\rho_i = \sum_{j=1}^N m_j W(|\mathbf{r}_{ij}|, h_i) \longrightarrow$ **Continuity equation automatically fulfilled.**

$\longrightarrow P_i = (\gamma - 1)\rho_i u_i$

Euler equation

$$\frac{d\mathbf{v}_i}{dt} = - \sum_{j=1}^N m_j \left(\frac{P_i}{\rho_i^2} + \frac{P_j}{\rho_j^2} \right) \nabla_i \bar{W}_{ij}$$

Artificial viscosity

First law of thermodynamics

$$\frac{du_i}{dt} = \frac{1}{2} \sum_{j=1}^N m_j \left(\frac{P_i}{\rho_i^2} + \frac{P_j}{\rho_j^2} \right) \mathbf{v}_{ij} \cdot \nabla_i \bar{W}_{ij}$$

Smoothed particle hydrodynamics is governed by a set of ordinary differential equations

BASIC EQUATIONS OF SMOOTHED PARTICLE HYDRODYNAMICS

Each particle carries either the energy or the entropy per unit mass as independent variable

Density estimate $\rho_i = \sum_{j=1}^N m_j W(|\mathbf{r}_{ij}|, h_i) \longrightarrow$ **Continuity equation automatically fulfilled.**

$$\longrightarrow P_i = (\gamma - 1)\rho_i u_i$$

Euler equation

$$\frac{d\mathbf{v}_i}{dt} = - \sum_{j=1}^N m_j \left(\frac{P_i}{\rho_i^2} + \frac{P_j}{\rho_j^2} \right) \nabla_i \bar{W}_{ij}$$

$+ \Pi_{ij}$

Artificial viscosity

$\mathbf{f}(\Lambda) + \text{ES}$

First law of thermodynamics

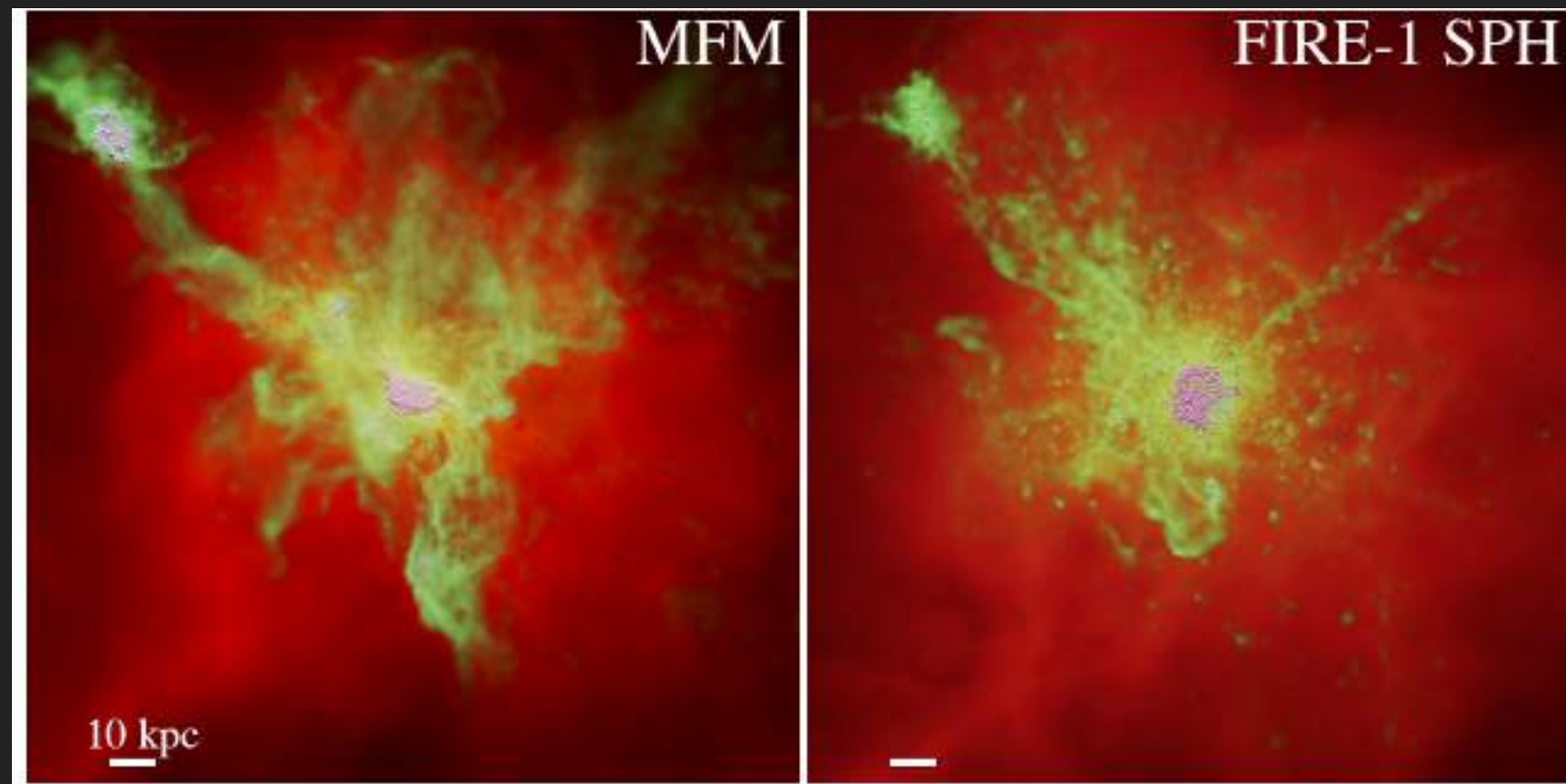
$$\frac{du_i}{dt} = \frac{1}{2} \sum_{j=1}^N m_j \left(\frac{P_i}{\rho_i^2} + \frac{P_j}{\rho_j^2} \right) \mathbf{v}_{ij} \cdot \nabla_i \bar{W}_{ij}$$

$+ \Pi_{ij}$

Numerical (Eulerian and Lagrangian) codes that include gravity, hydrodynamics and other processes have been developed in the last decades.

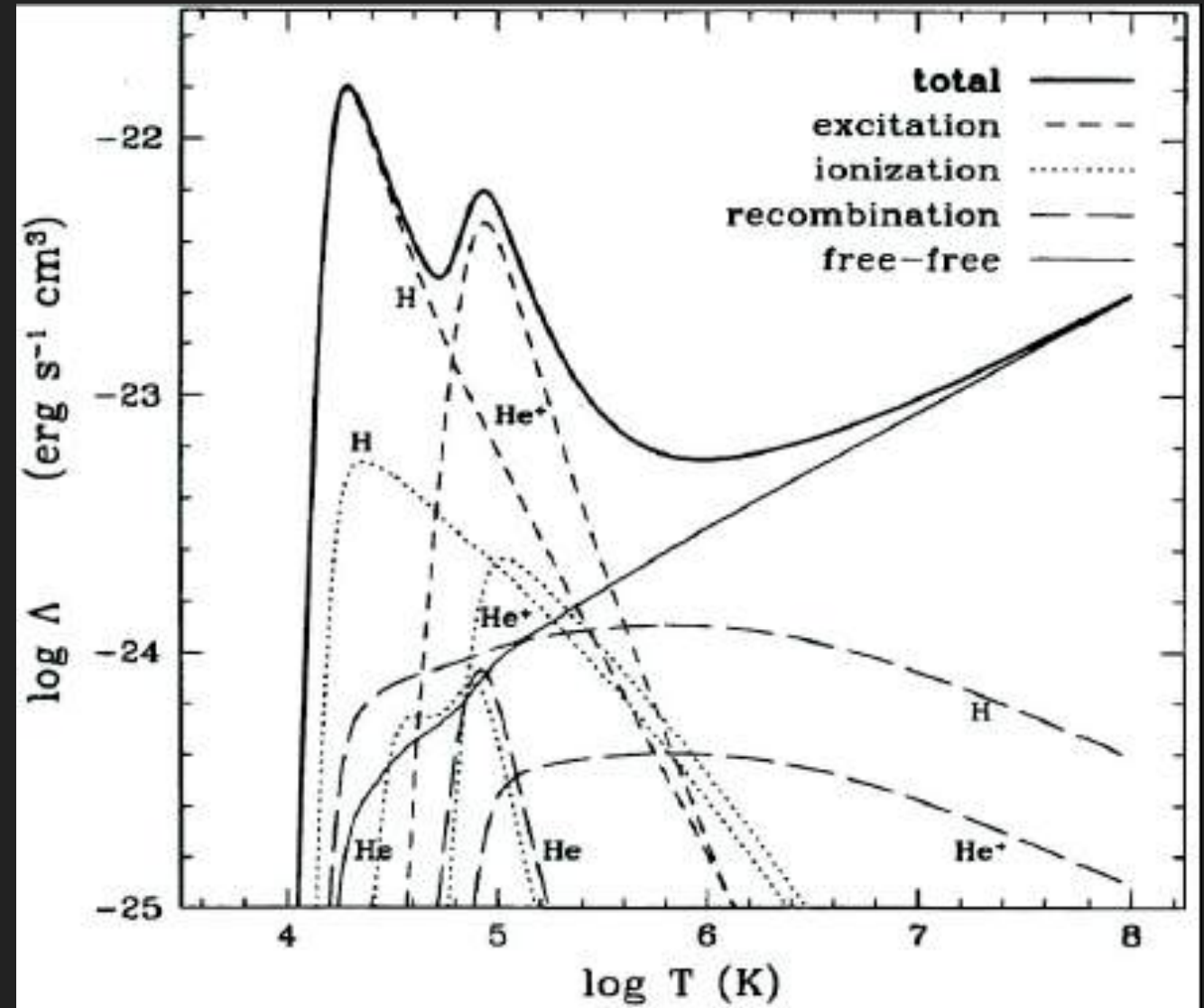
Smooth Particle Hydrodynamics (Gingold & Monaghan 1997, Lucy 1977) has proved to be a powerful technique to study the formation of the structure, particularly in a cosmological context because it has more flexibility to adapt to the non-linear growth of the structures

AREPO (Springel 2010) and **GIZMO** (Hopkins+2017) provide alternative new approaches.



The cooling rate depends on gas density and chemical composition.

$$t_{\text{cool}} \equiv \frac{\rho \mathcal{E}}{\mathcal{L}} = \frac{3nk_{\text{B}}T}{2n_{\text{H}}^2 \Lambda(T)} \approx 3.3 \times 10^9 \frac{T_6}{n_{-3} \Lambda_{-23}(T)} \text{ yr},$$

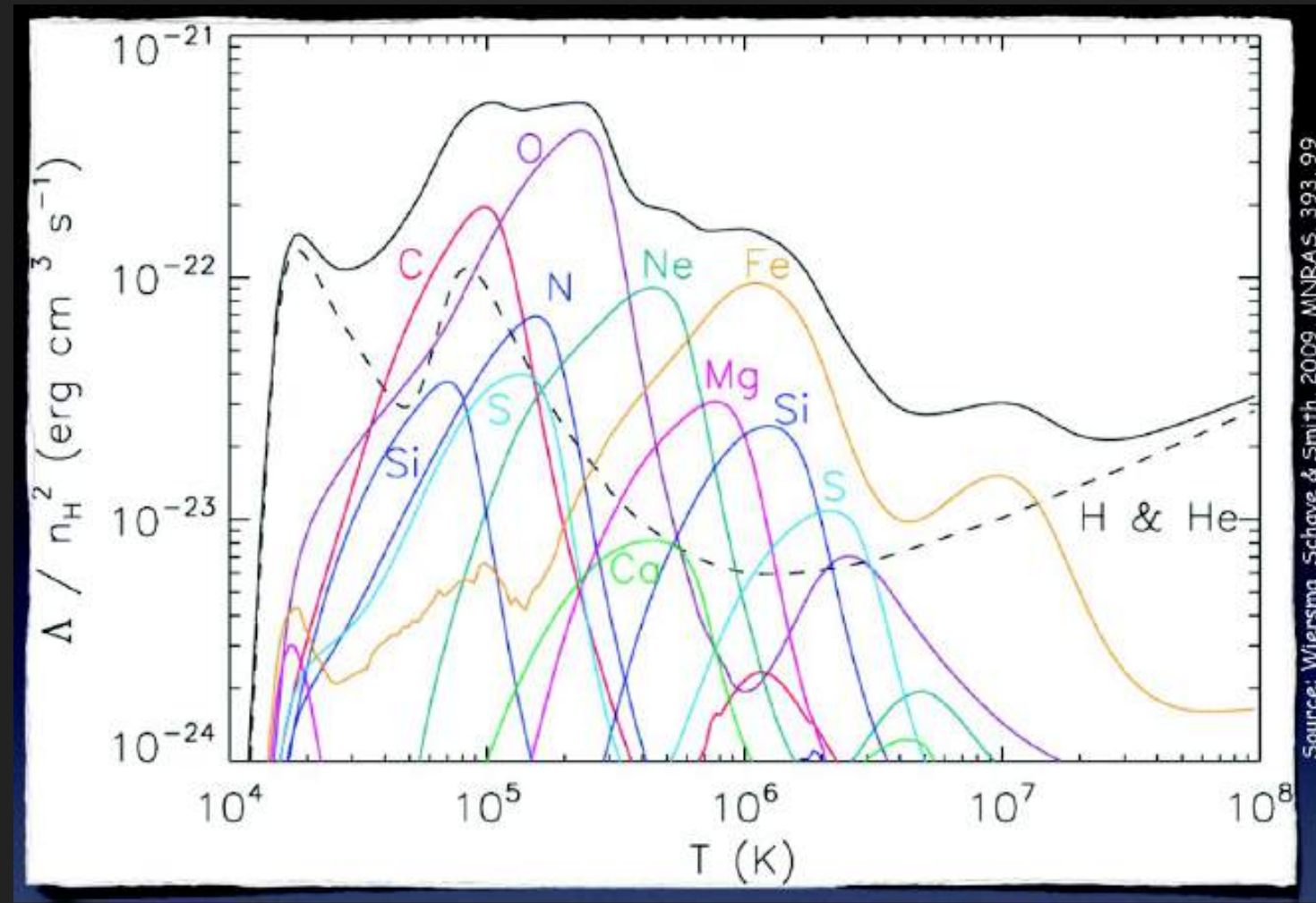


Katz et al. 1996

assuming collisional ionization equilibrium

Most current cosmological codes include metal-enrichment and metal-dependent radiation equilibrium cooling (e.g. Mosconi +2001; Lia+2002; Kravtov2003; Scannapieco+2005; Oppenheimer+2016; Tornatore+2007; Ceverino+2009; Wiersman+2009; Vogelsberger+2013).

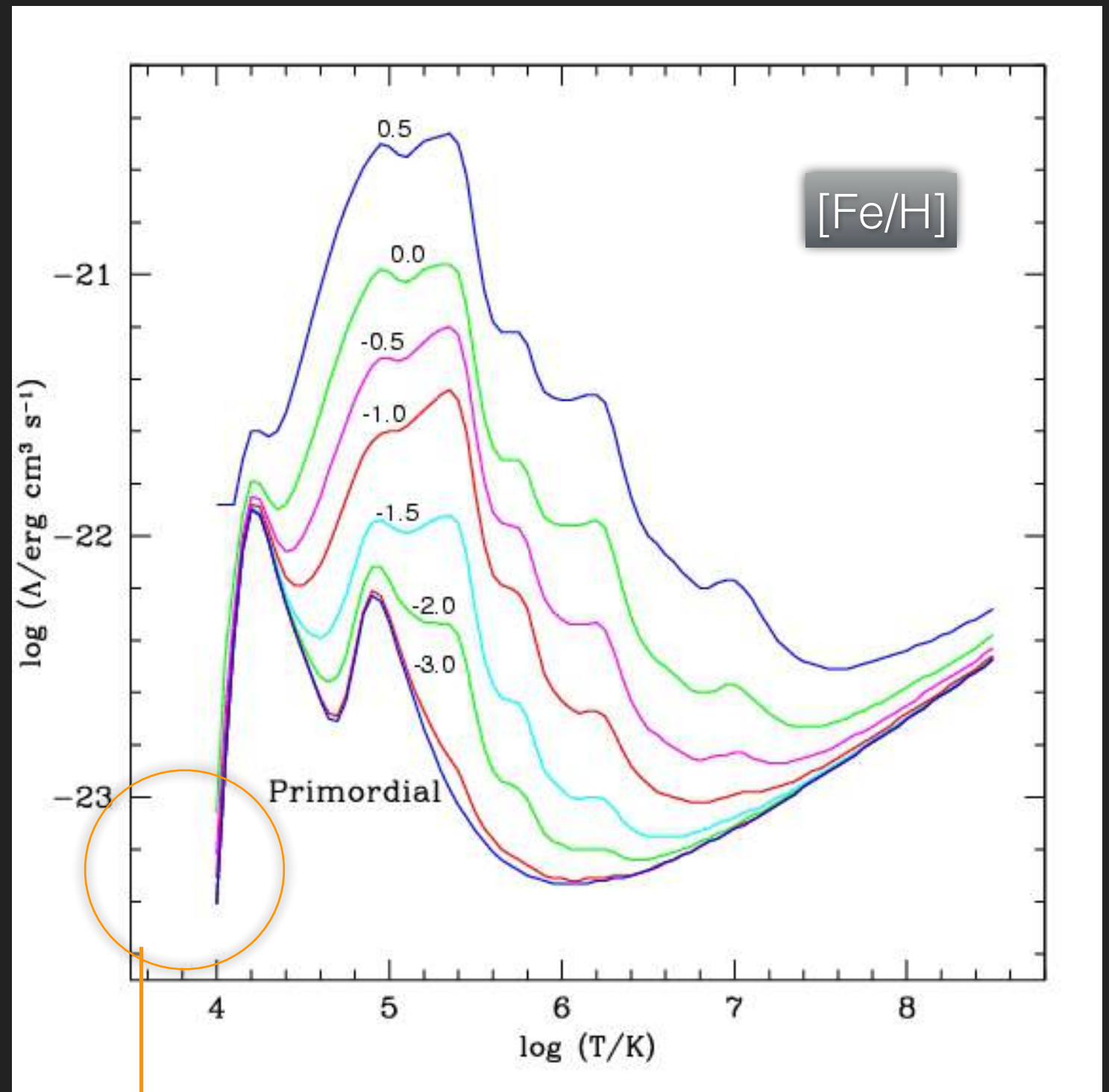
Non-equilibrium cooling for regions where gas cools down very efficient (or the radiation field changes rapidly) are being explored in galaxy-scale simulations (e.g. Ritching et al. 2014; Hu+2016; Ritching & Schaye 2016).



The chemical abundances of gas phase is crucial to estimate the cooling rates correctly (e.g. Mosconi+2001)

How metals are mixed in the ISM, CGM and IGM affect the evolution of the different gas-phases.

$$t_{\text{cool}} \equiv \frac{\rho \mathcal{E}}{\mathcal{C}} = \frac{3nk_{\text{B}}T}{2n_{\text{H}}^2\Lambda(T)} \approx 3.3 \times 10^9 \frac{T_6}{n_{-3}\Lambda_{-23}(T)} \text{yr},$$



$T < 10^4 \text{ K} \rightarrow$ molecular cooling + metal cooling in non-equilibrium

The transformation of gas into stars involves physical processes acting in spatial and time scales that are not resolved in cosmological simulations. The complexity of the interstellar medium is also difficult to represent in these simulations.

Subgrid modelling is an approach that intent to model the effects of physical processes acting on unresolved scales on those scales are numerical resolved.

The transformation of gas into stars involves physical processes acting in spatial and time scales that are not resolved in cosmological simulations. The complexity of the interstellar medium is also difficult to represent in these simulations.

Subgrid modelling is an approach that intent to model the effects of physical processes acting on unresolved scales on those scales are numerical resolved.

Star formation schemes are in general quite simple and based on the Schimdt relation (Schimdt 1959):

$$\rho_{\text{star}} \sim \rho_{\text{gas}} / \tau_c$$

τ_c is a characteristic time. In general it is assumed to be the dynamical time:

$$t_{\text{dyn}} = \sqrt{3\pi/16G\bar{\rho}}$$

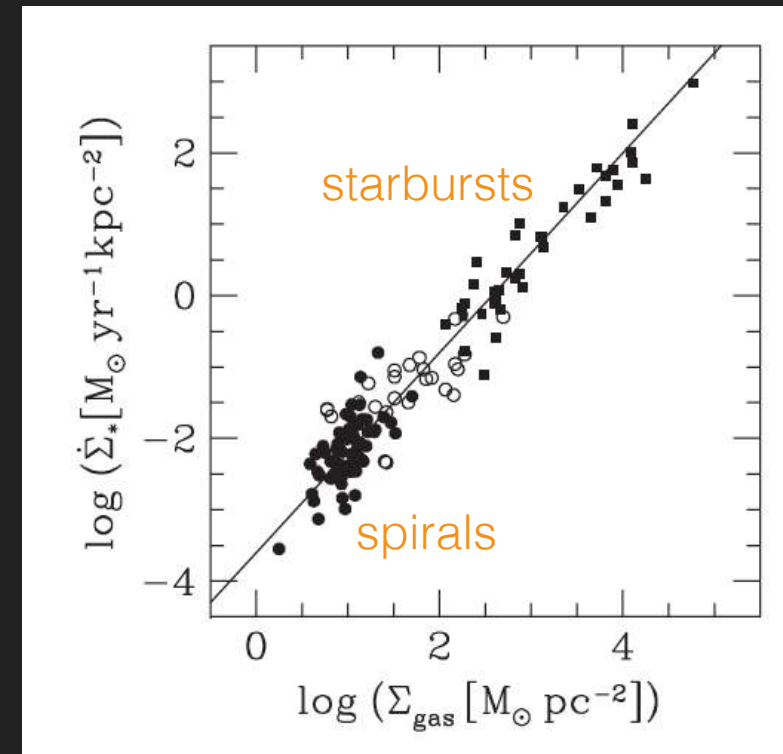
$$\dot{\Sigma}_* = (2.5 \pm 0.7) \times 10^{-4} \left(\frac{\Sigma_{\text{gas}}}{M_{\odot} \text{pc}^{-2}} \right)^{1.4 \pm 0.15} M_{\odot} \text{yr}^{-1} \text{kpc}^{-2}$$

In general, gas above a certain **density threshold and temperature (n)** is eligible for star formation:

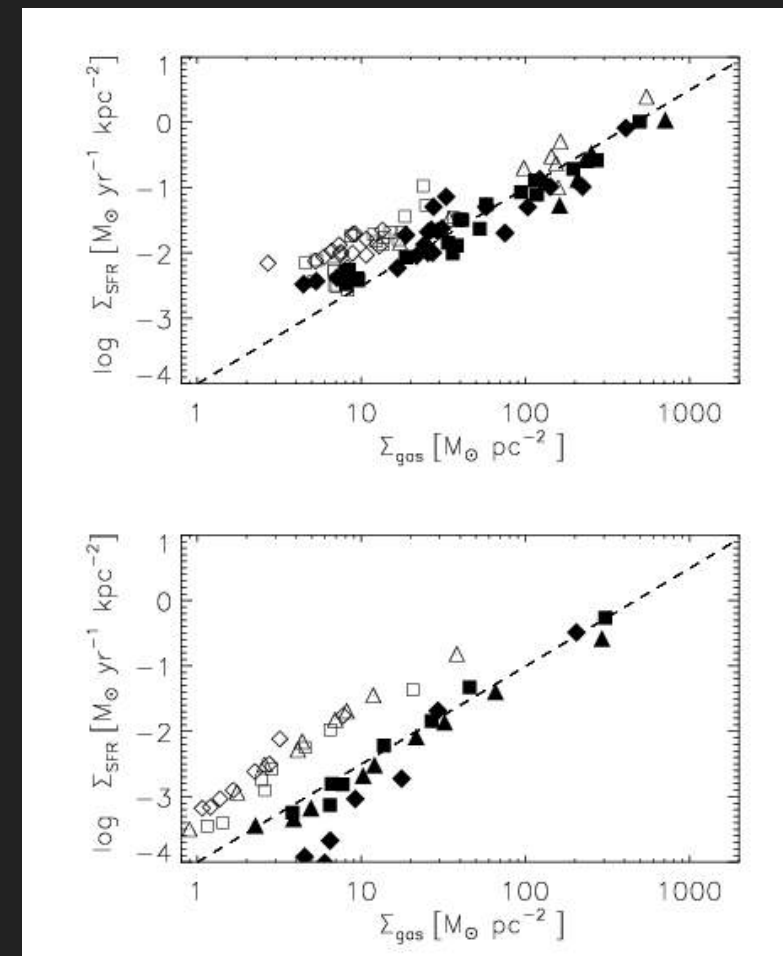
$$\rho_{\text{star}} = \epsilon \rho_{\text{gas}}^{1.5}$$

where ϵ is the efficiency of star formation and is adjusted to reproduce the observed KS law that relates the star formation surface density with the gas surface density (Kennicutt 1998).

See Schaye+2015, Hopkins+2018 (and references there in) for different star formation implementations.

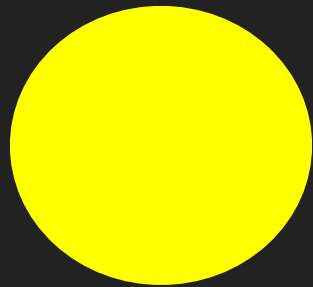


Kennicutt+1998

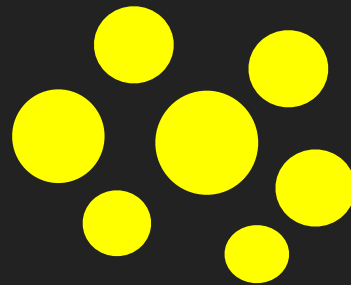


Scannapieco+2006

Numerical space



Physical space



Need

IMF:
SNe / long-lived stars

Type II SNe

Mstar > 8 Msun,
typical life-times
~10⁶ yr
Produce most O, Si,
Ca, etc

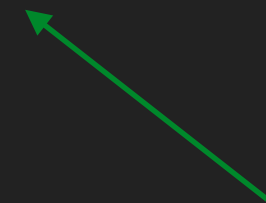
Type Ia SNe

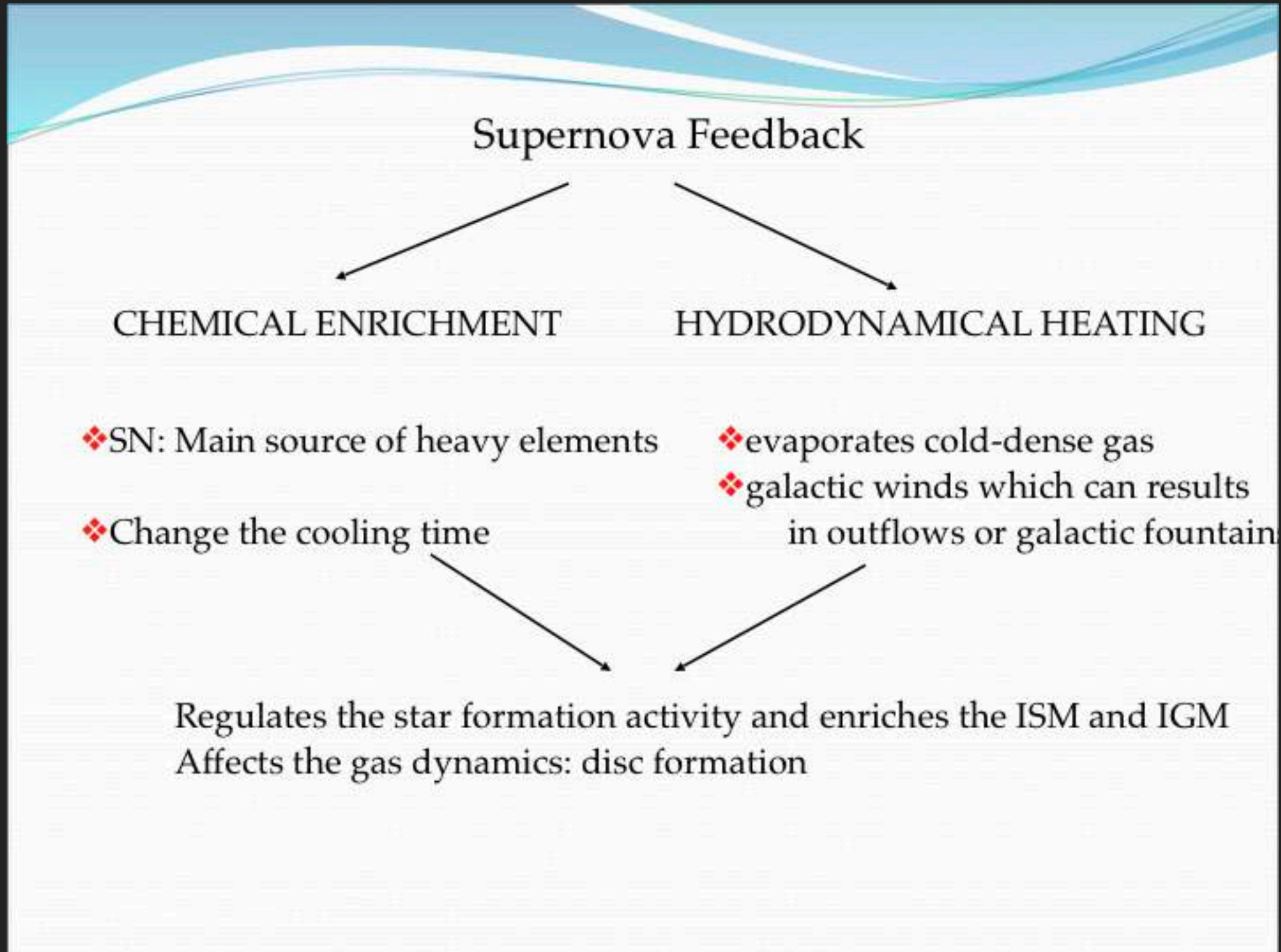
Intermediate stars/binary
systems
typical life-times ~1 Gyr
Produce most Fe

AGBs

Intermediate stars
life-times ~1-2 Gyr
C, N

Nucleosynthesis
yields





When SN explosions take place, metals are distributed according to the SPH technique (Mosconi+2001). For a given chemical element x at a particle i ,

$$Mx_i = \sum_j m_j / \rho_j Mx_i W(r_{ij}, h_{ij})$$

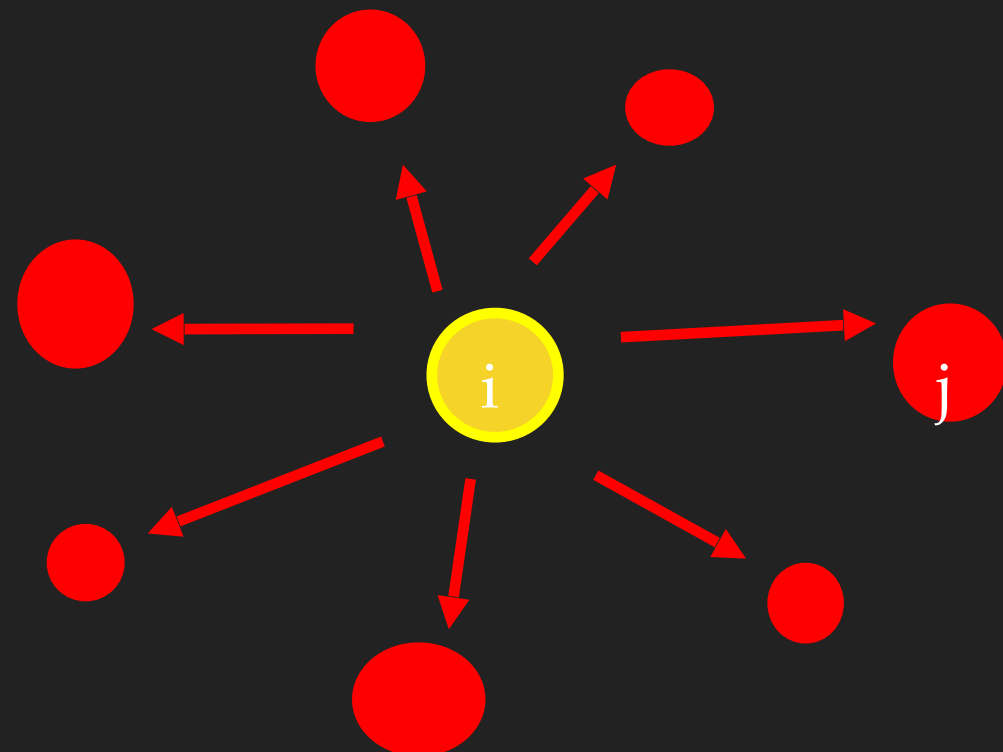
Neighbours will receive

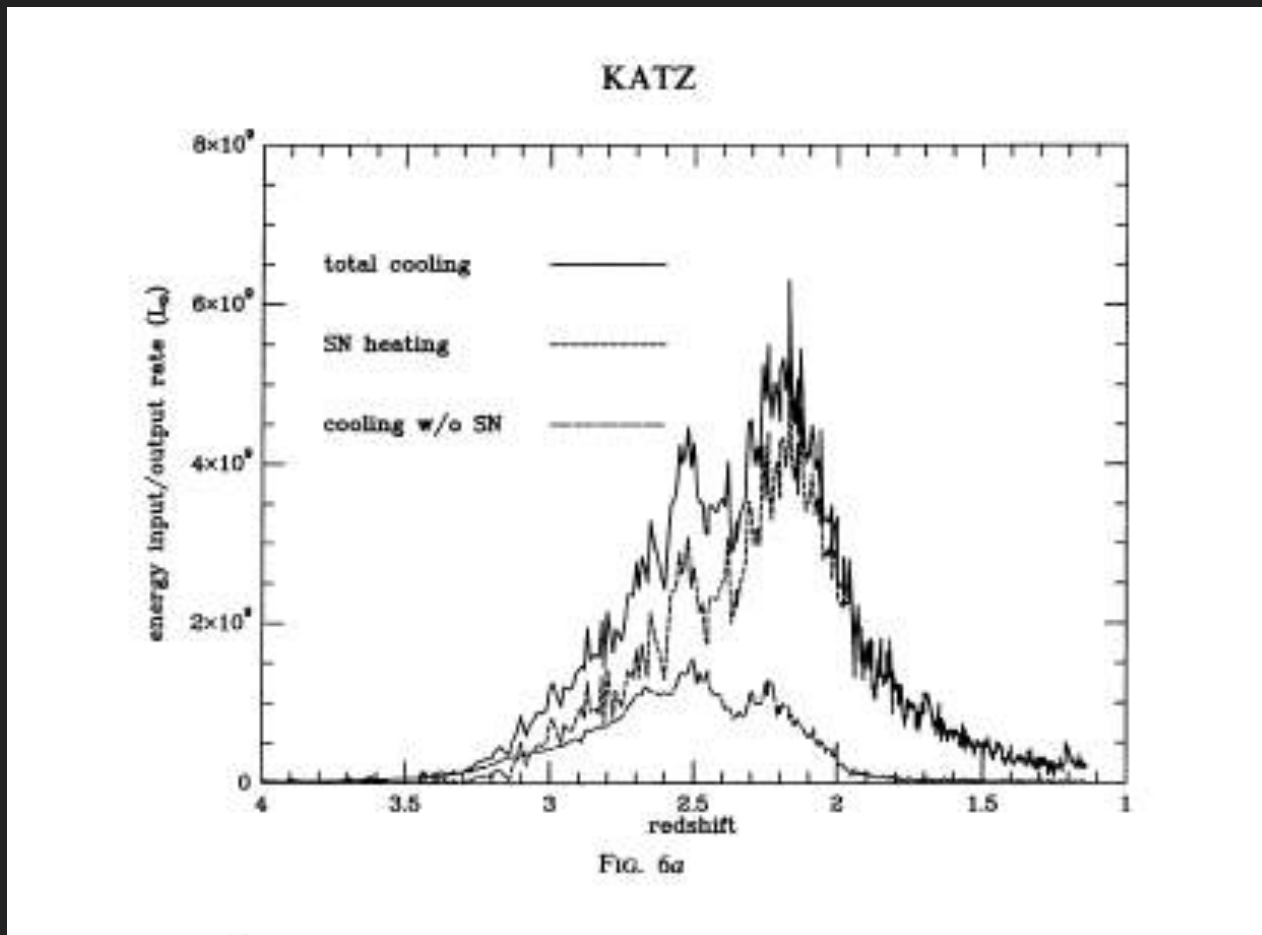
$$Mx_j = m_j / \rho_j Mx_i W(r_{ij}, h_{ij})$$

Exploding star particle

Gaseous neighbours

Metal diffusion?



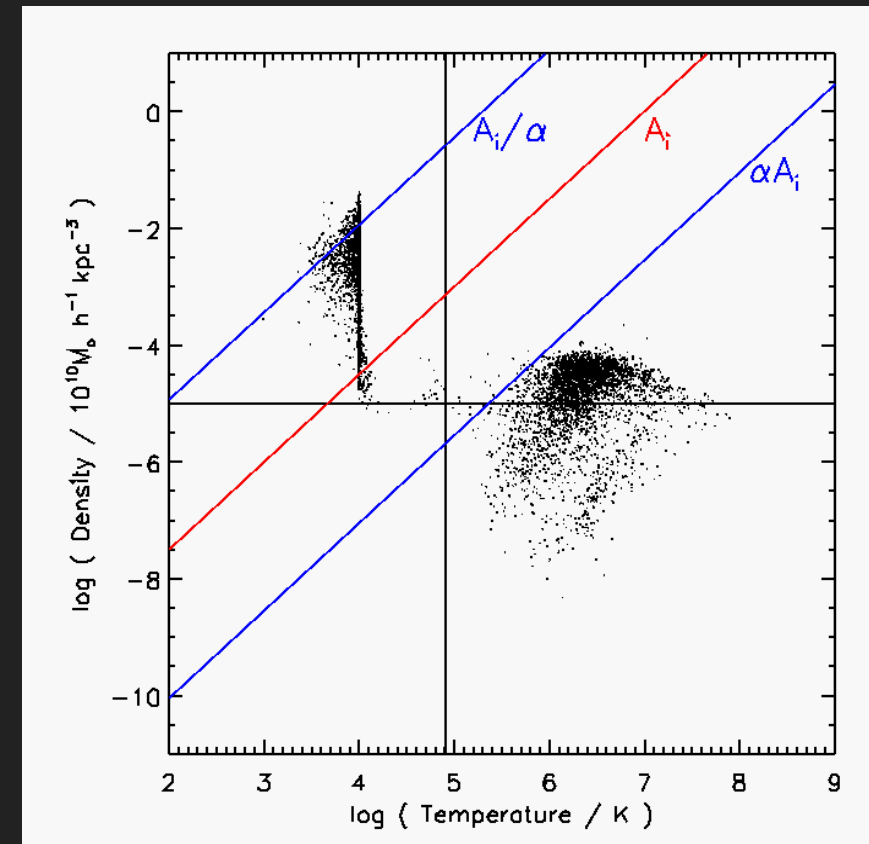


Thermal feedback:
 injection of SN energy
 directly into the ISM
 directly →
 it is radiated away very
 efficiently

$$t_{\text{cool}} \equiv \frac{\rho \mathcal{E}}{\mathcal{C}} = \frac{3nk_B T}{2n_H^2 \Lambda(T)} \approx 3.3 \times 10^9 \frac{T_6}{n_{-3} \Lambda_{-23}(T)} \text{ yr,}$$

The energy is injected mainly in high density regions with short cooling times compared to the typical time step of integration (overcooling):

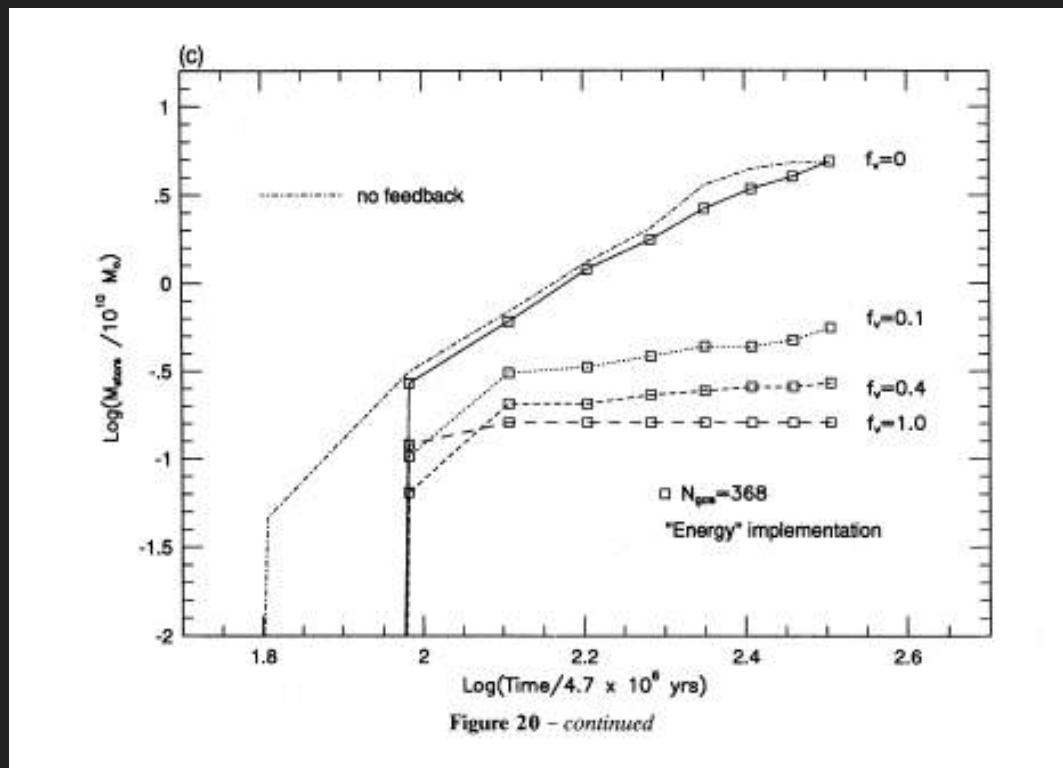
There is no time for this energy to modify the dynamics.



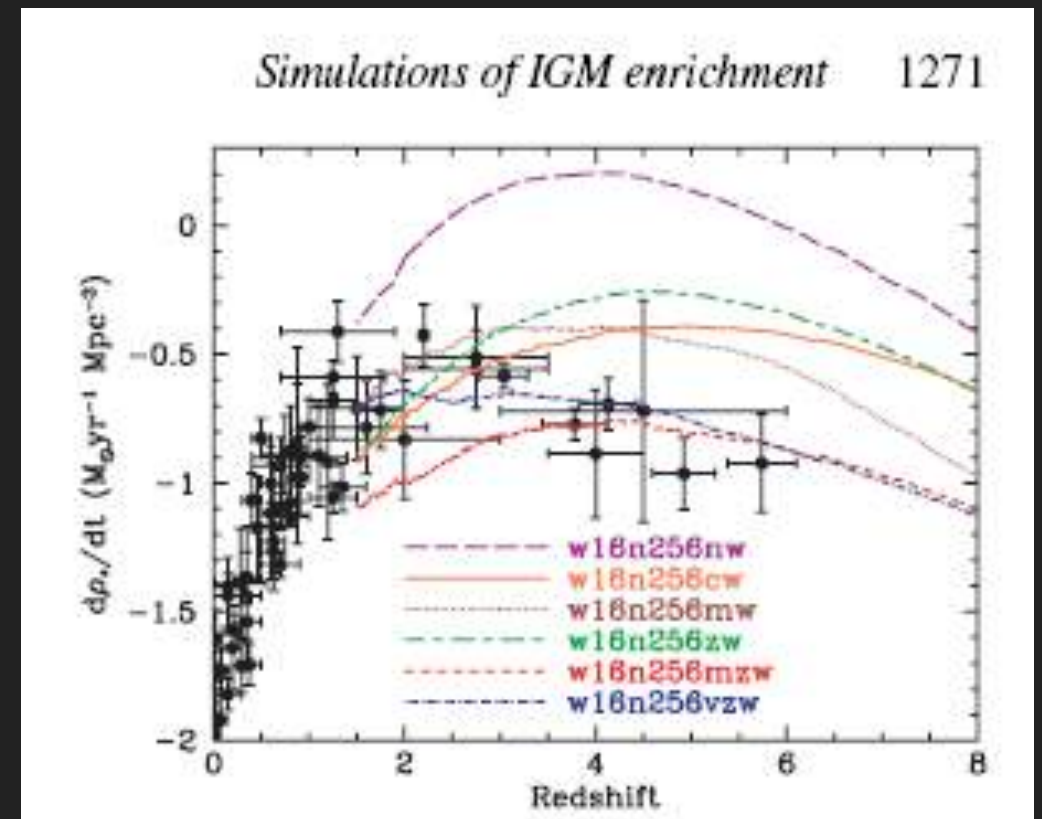
Alternative implementations show that strong stellar feedback can modulate the star formation and

First ad hoc solution was kicking particles: a fraction of SN energy is dumped as thermal energy and the remaining one as kinetic energy as proposed by Navarro & White (1993).

Momentum-driven wind model:
 wind velocity scales with the velocity dispersion of stars ($v_{\text{wind}} \propto \sigma$)
 the momentum input scales with the star-formation rate
 the **mass-loading factor** (the ratio of the wind mass loss to the star formation rate) is inversely proportional to the velocity dispersion



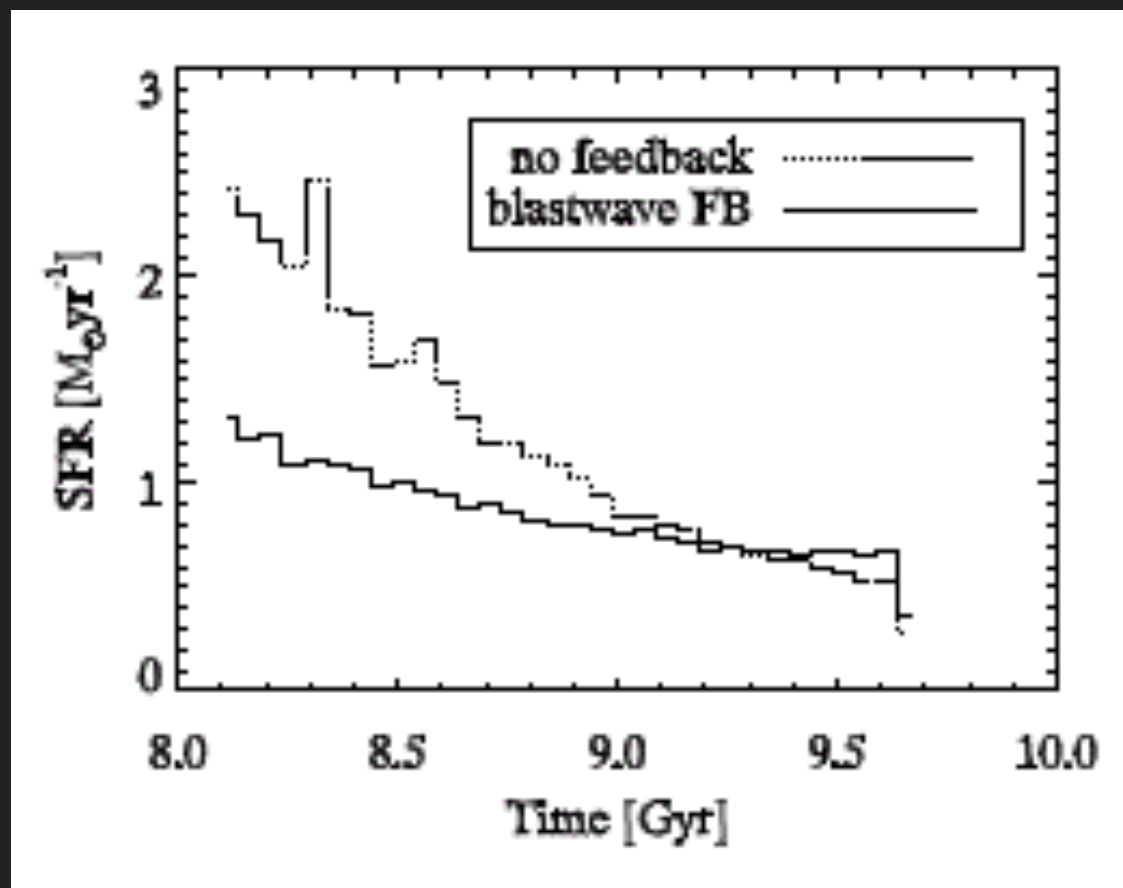
Navarro & White 1993



Oppenheimer & Davé 2006

Gerritsen (1997) and Thacker & Couchman (2000) explored the effects of turning off the cooling for certain selected particles. The model has to decide which particles will be affected and for how long, introducing ad hoc parameters.

Stinson et al. (2006), followed this model and extended by using the blast wave solution of Chevalier (1974) and McKee & Ostriker (1977) to estimate the maximum radius and the time.



Stinson et al. 2006

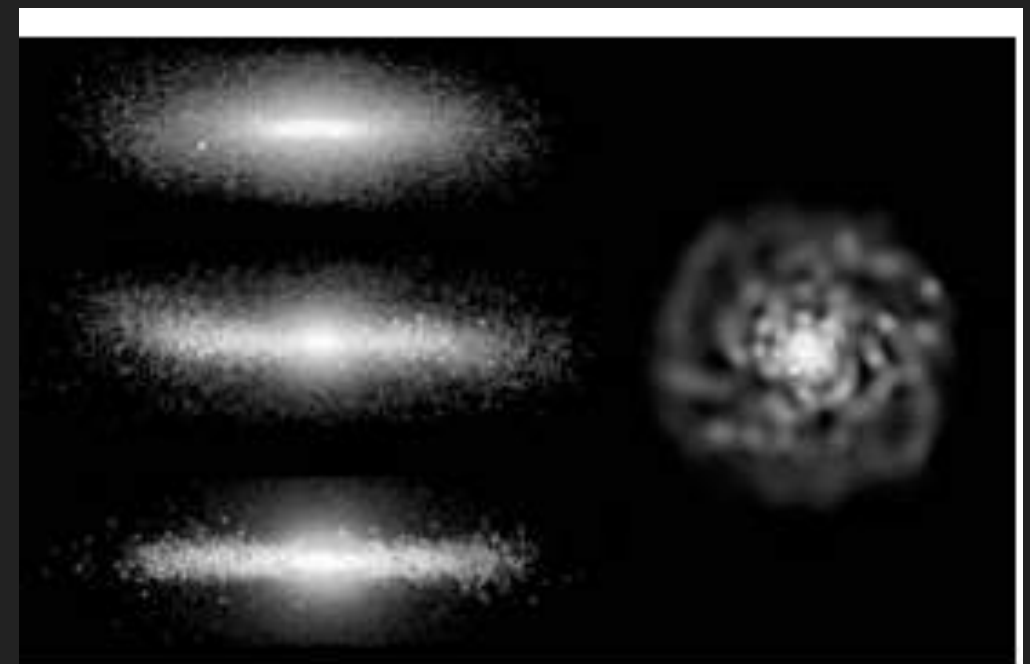
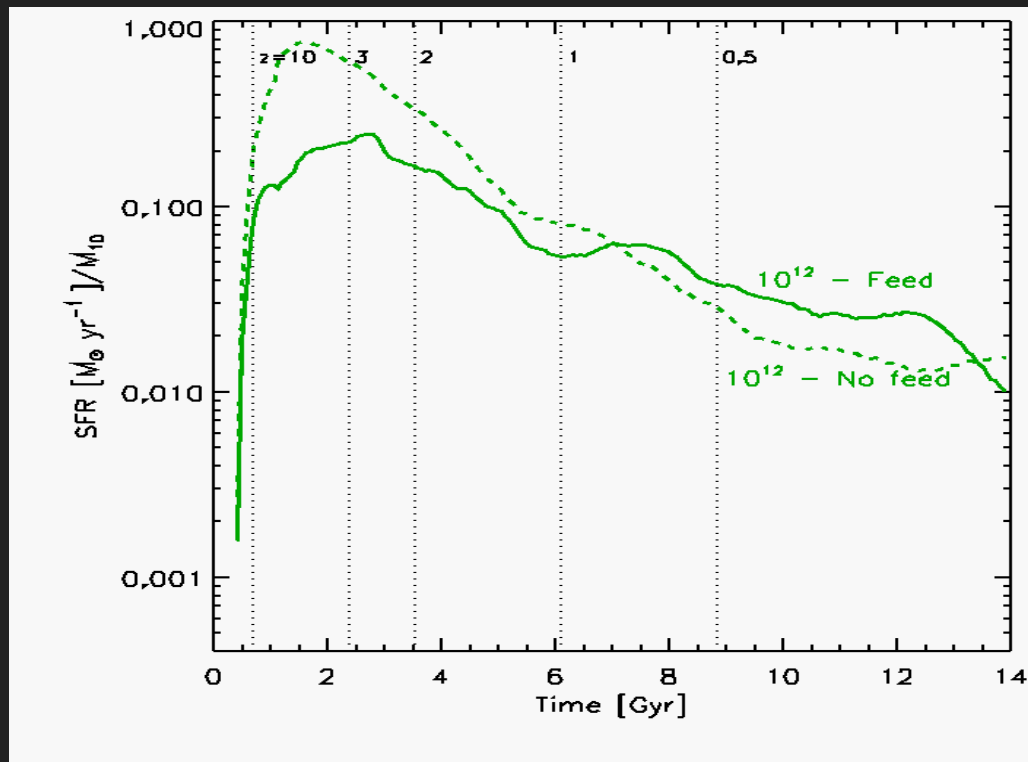
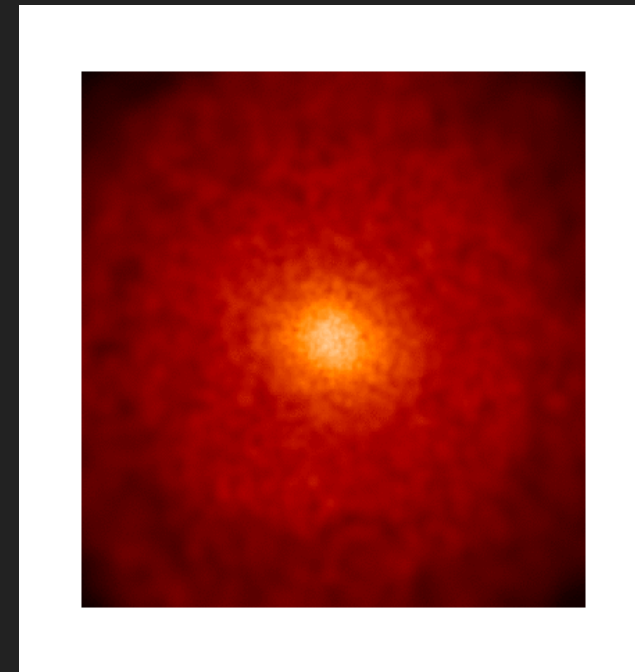


Figure 6. Left-hand panel: brightness maps of the edge-on discs of (from top to bottom) GAL1, MW1 and DWF1 at $z = 0$. Each star particle in the simulations has been weighted by its age-dependent bolometric luminosity. Right-hand panel: the face-on surface density of the gas for DWF1 at $z = 0$. Each frame is 30 kpc across.

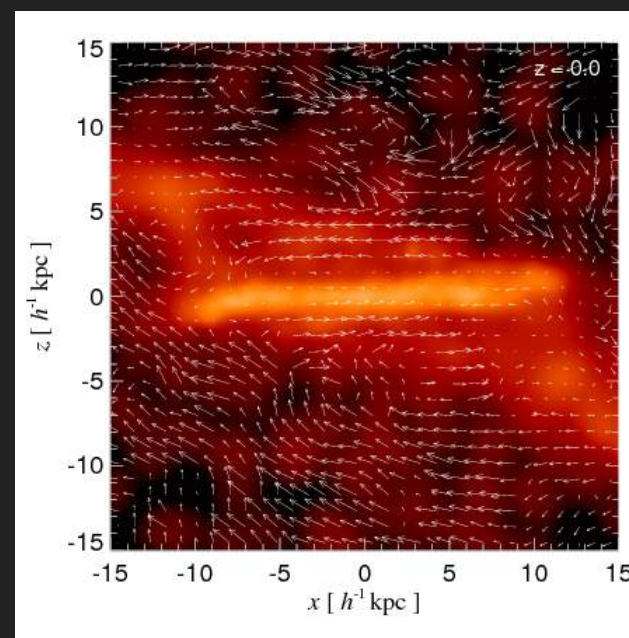
Governato et al. 2006



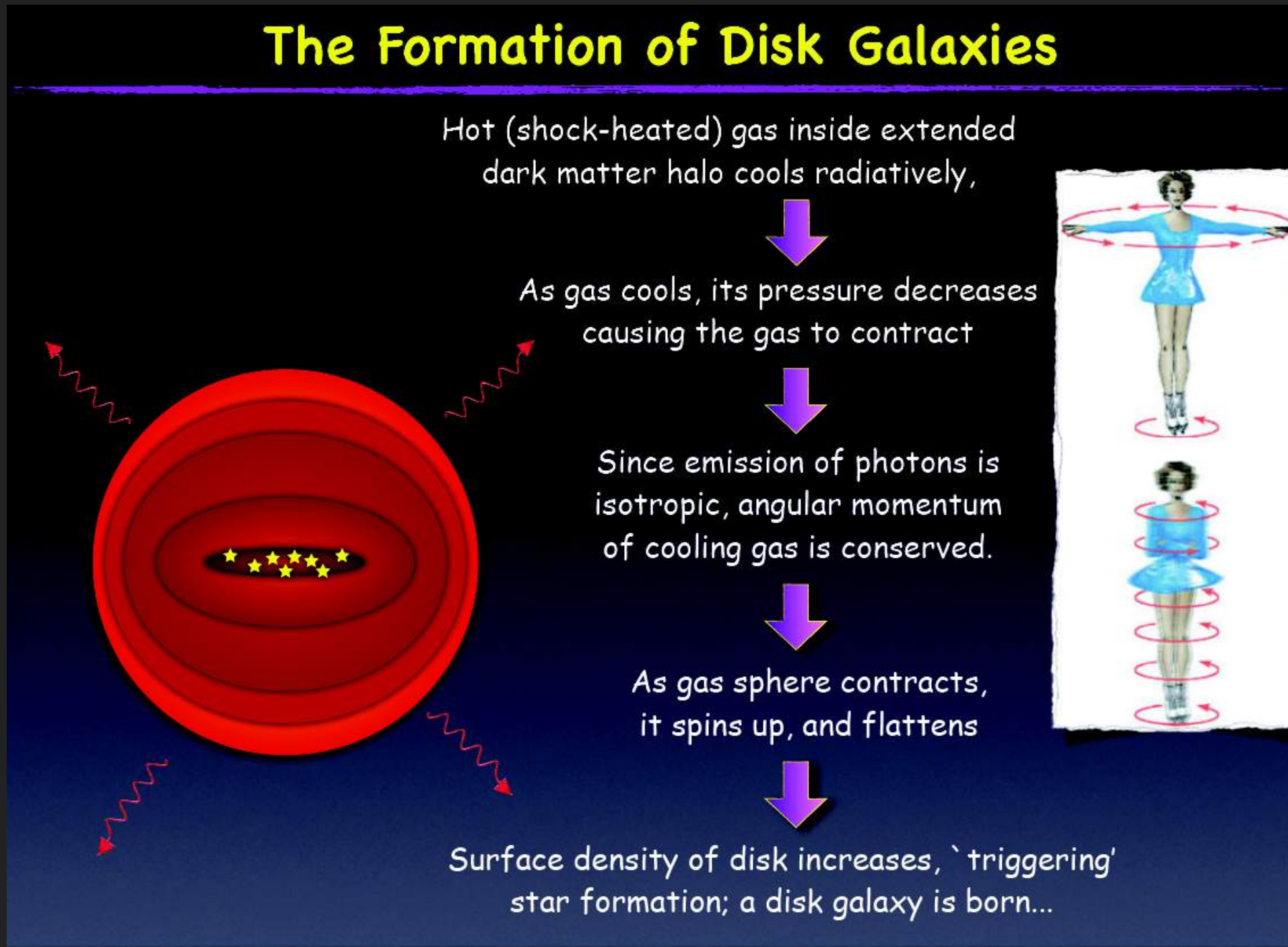
no feedback



feedback

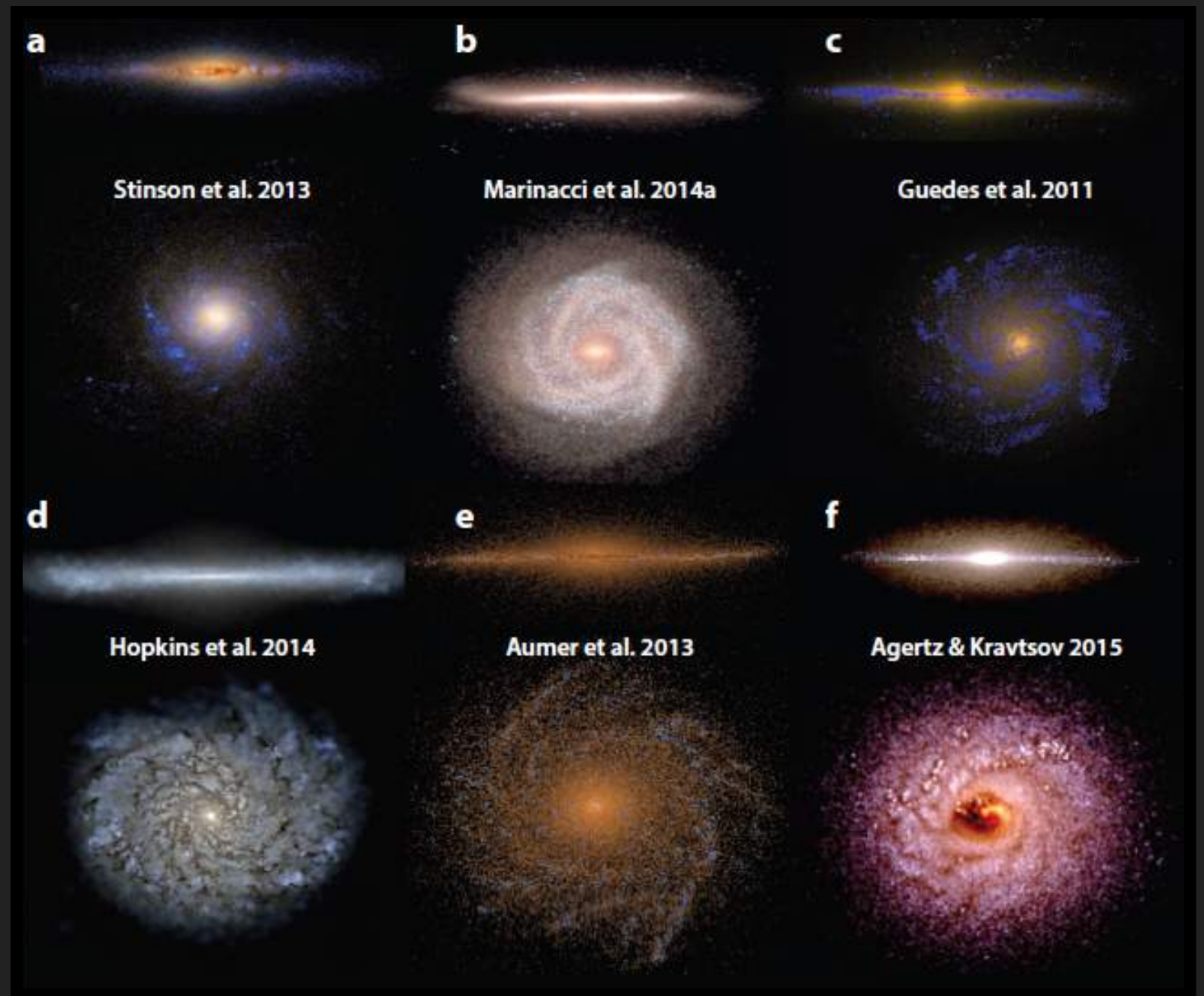


Two-phase approach: hot and cold gas phases are evolved separately. SN energy is stored in cold phase until reaching the entropy of the hot phase (Scannapieco et al. 2006)



The improvement of the subgrid physics related to stellar feedback:

- prevents the overcooling and early transformation of gas into stars.
- the formation of gas reservoir (with high angular momentum) to be accreted later at lower redshift.
- extended discs can form that reproduce the size-mass relation and have the expected angular momentum content, on average.

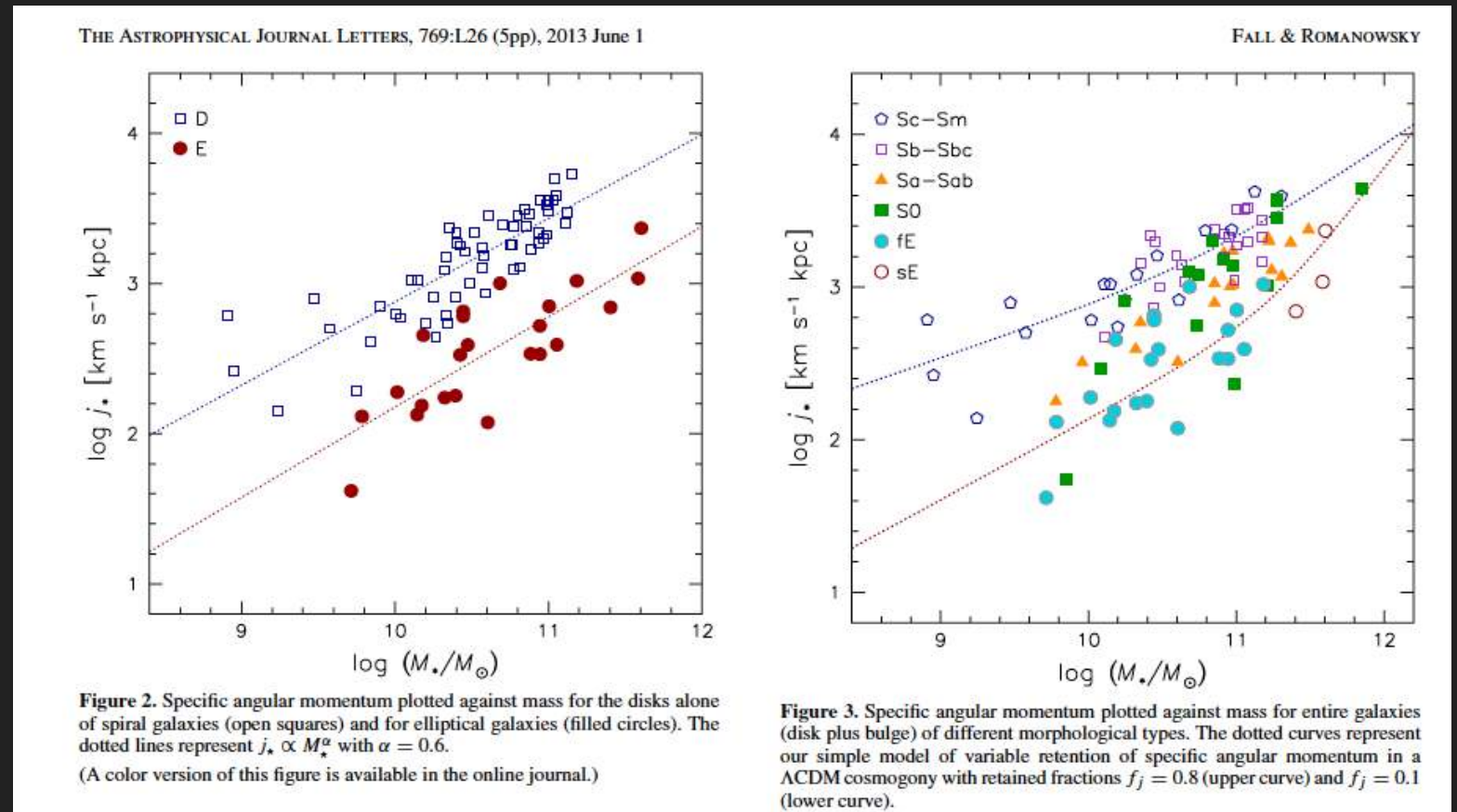


$$\lambda = \frac{J |E|^{1/2}}{G M^{5/2}}$$

$J/M = \text{cte} \times M^\alpha \quad \alpha \sim 0.6$
 The trend is consistent with the theoretical expectations for spin parameter $\lambda \sim 0.037$.

The specific angular momentum ($j=J/M$) of baryons in discs is similar to that of the dark matter.

Hydrodynamical simulations show a **global** angular momentum conservation for discs (Pedrosa & Tissera 2015; see also Telku+2015,Lagos+2017)



$J/M = \text{cte} \times M^\alpha \quad \alpha \sim 0.6$
 The trend is consistent with the theoretical expectations for $\lambda \sim 0.037$.

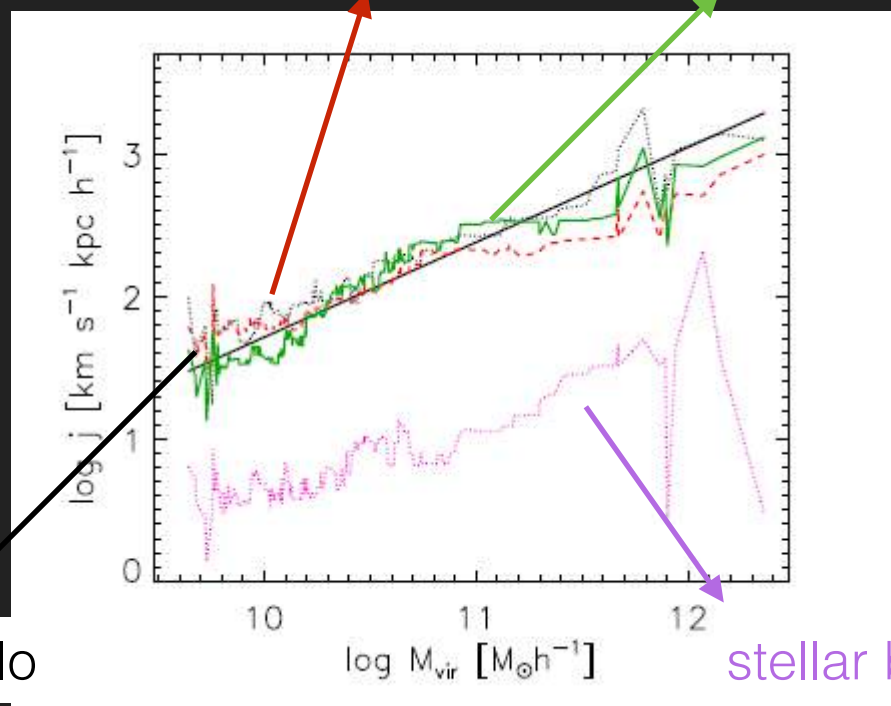
$$\lambda = \frac{J |E|^{1/2}}{G M^{5/2}}$$

The specific angular momentum ($j=J/M$) of baryons in discs is similar to that of the dark matter.

Hydrodynamical simulations show a **global** angular momentum conservation for discs (Pedrosa+2015; see also Telku+2015, Lagos+2017)

stellar discs

gaseous discs



dark matter halo

stellar bulges

THE ASTROPHYSICAL JOURNAL LETTERS, 769:L26 (5pp), 2013 June 1

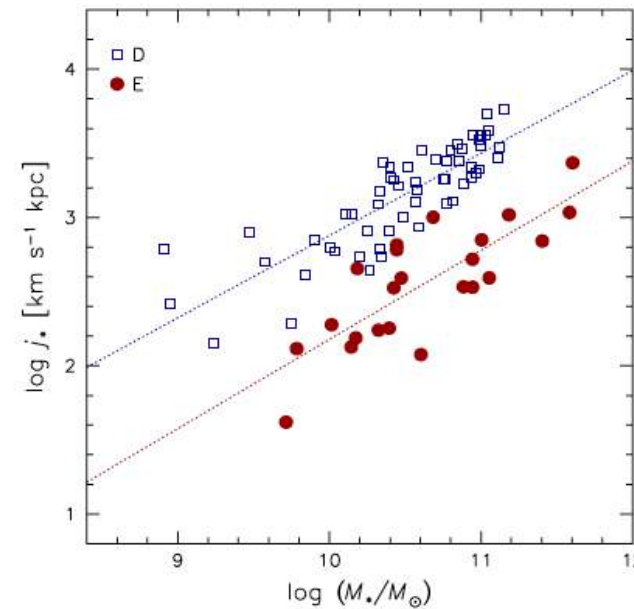


Figure 2. Specific angular momentum plotted against mass for the disks alone of spiral galaxies (open squares) and for elliptical galaxies (filled circles). The dotted lines represent $j_* \propto M_*^\alpha$ with $\alpha = 0.6$. (A color version of this figure is available in the online journal.)

FALL & ROMANOWSKY

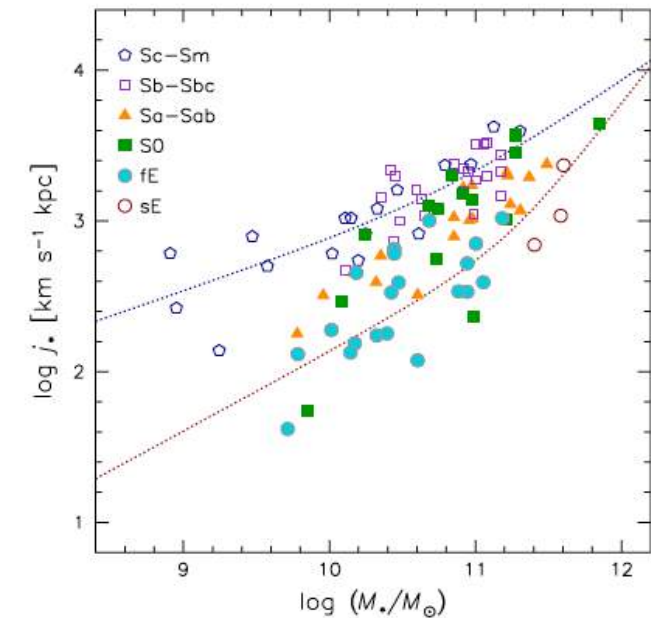
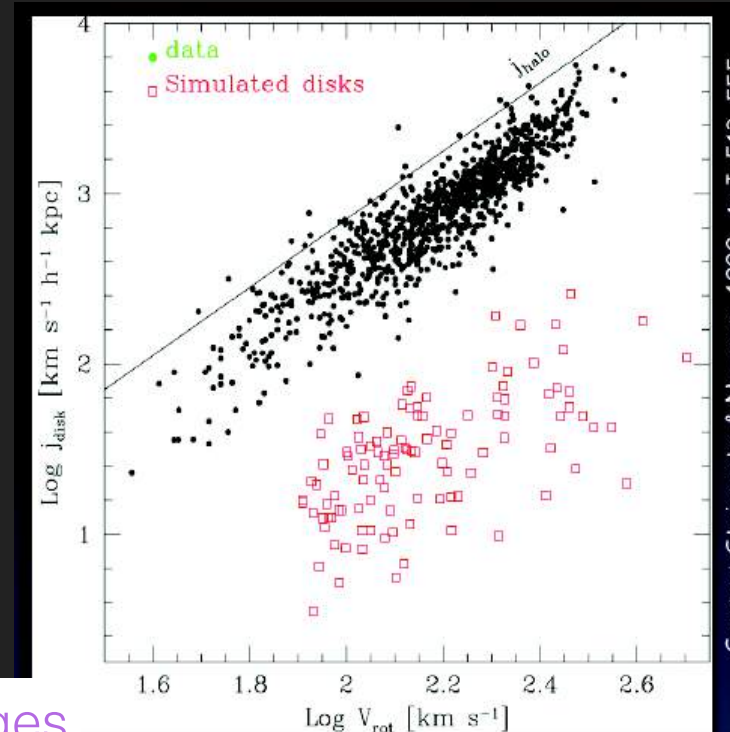


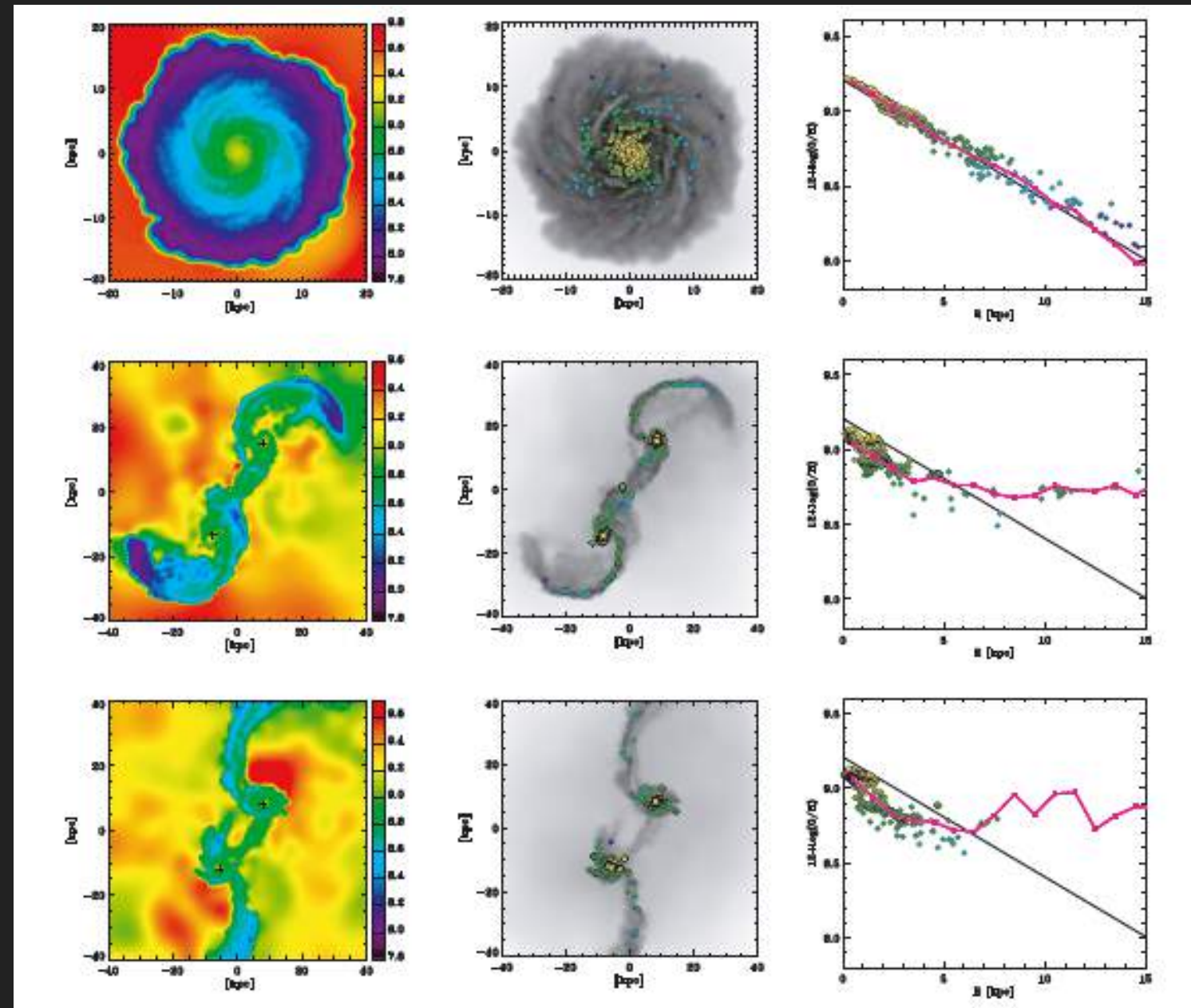
Figure 3. Specific angular momentum plotted against mass for entire galaxies (disk plus bulge) of different morphological types. The dotted curves represent our simple model of variable retention of specific angular momentum in a Λ CDM cosmology with retained fractions $f_j = 0.8$ (upper curve) and $f_j = 0.1$ (lower curve).

Pedrosa & Tissera 2015



Source: Steinmetz & Navarro, 1999, ApJ, 513, 555

Perez et al. 2011



Cosmological simulations provide the global environmental effect naturally: mergers rates and configurations the interaction of galaxies and with the CGM /IGM.

Mergers have been reported to:

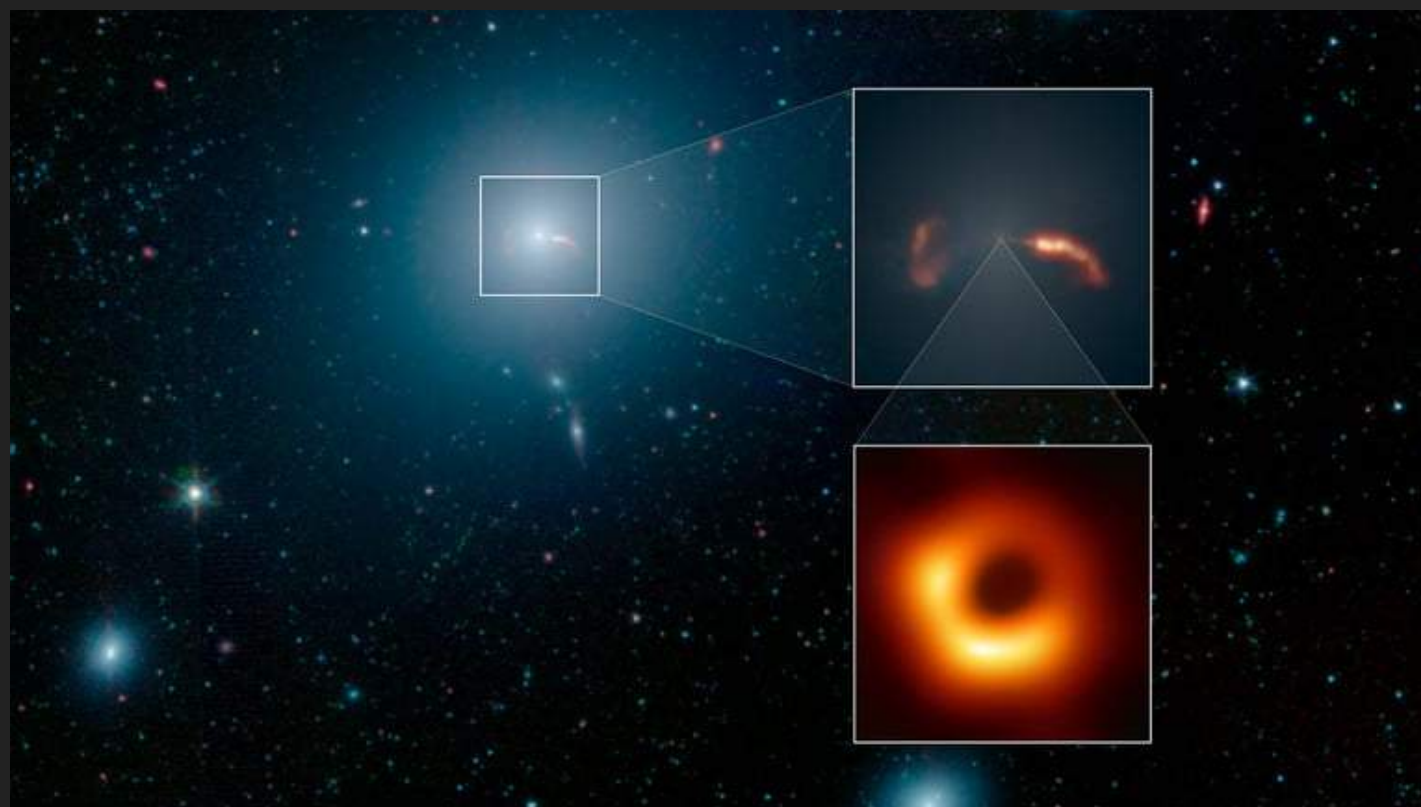
- induce bars (secular evolution);
- drive starbursts
- mix chemical elements
-

metallicity distribution star-formation region metallicity gradients

Massive bulge-dominated galaxies have larger escape velocities and hence galactic outflows are less efficient at regulating the star formation.

They are more massive than observed → AGN feedback is required (Croton+2006).

Simulations reproduce bulge-dominated galaxies with structural properties in global agreement with observations (Kobayashi 2004, 2005; Johansson+2012)



Possible two-phase formation scenario:

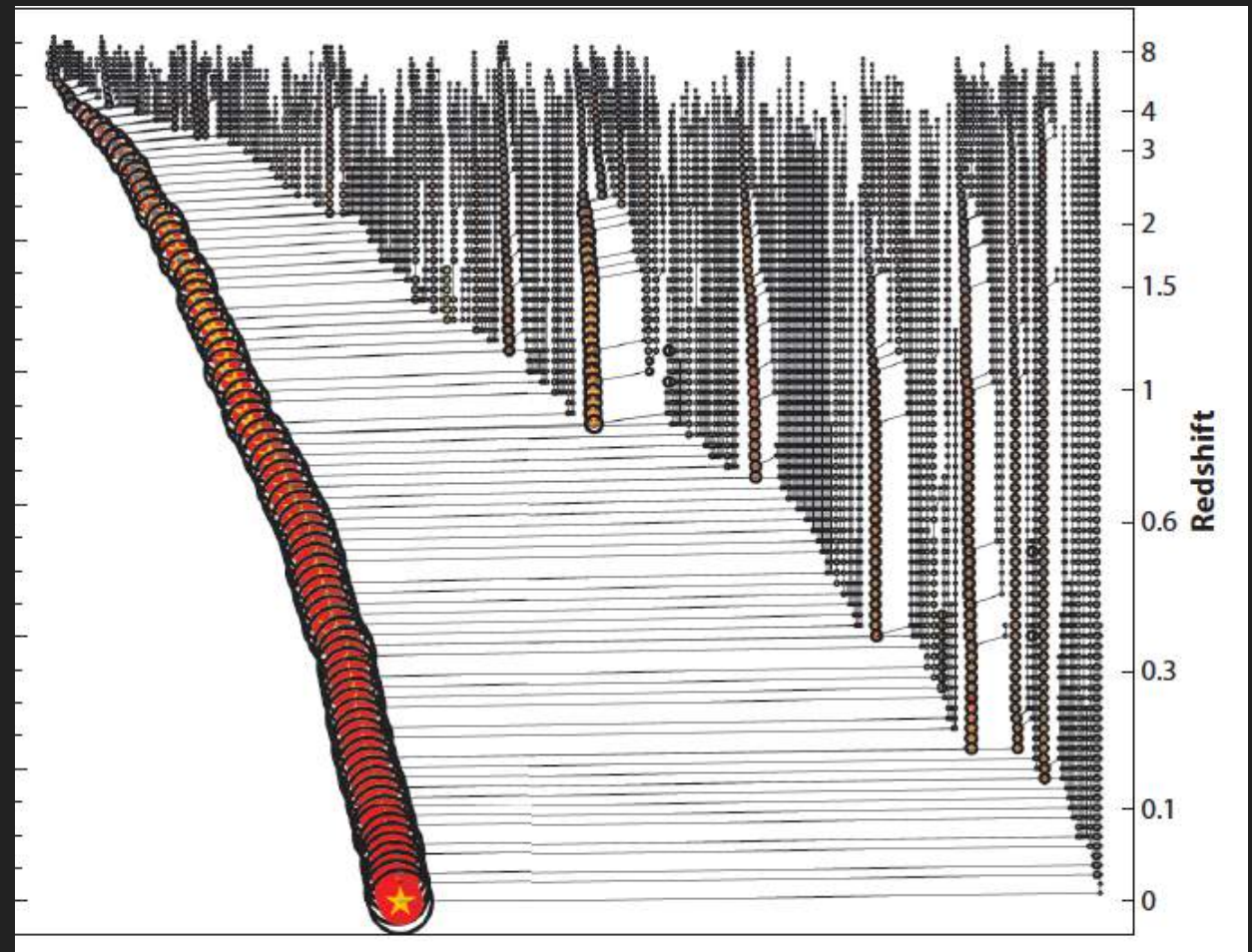
Phase 1: At $z > 1.5$ galaxies grow by in situ star formation in the deep potential well of massive dark matter haloes.

Gas is efficiently transformed into stars —
 $>$ galaxies are compact.

Major merger can take place.

Phase 2: star formation is quenched because gas inflows cannot easily penetrate the hot gas haloes (CGM; Birnboim & Dekel 2003).

Mergers continue to feed galaxies via dry mergers, being larger more massive systems (Rogríguez-Gomez+2016). The contribution of accreted stellar populations is important principally in the external regions. They are expected to contribute to increase the mass and size of galaxies (Naab 2009).



Naab+2014

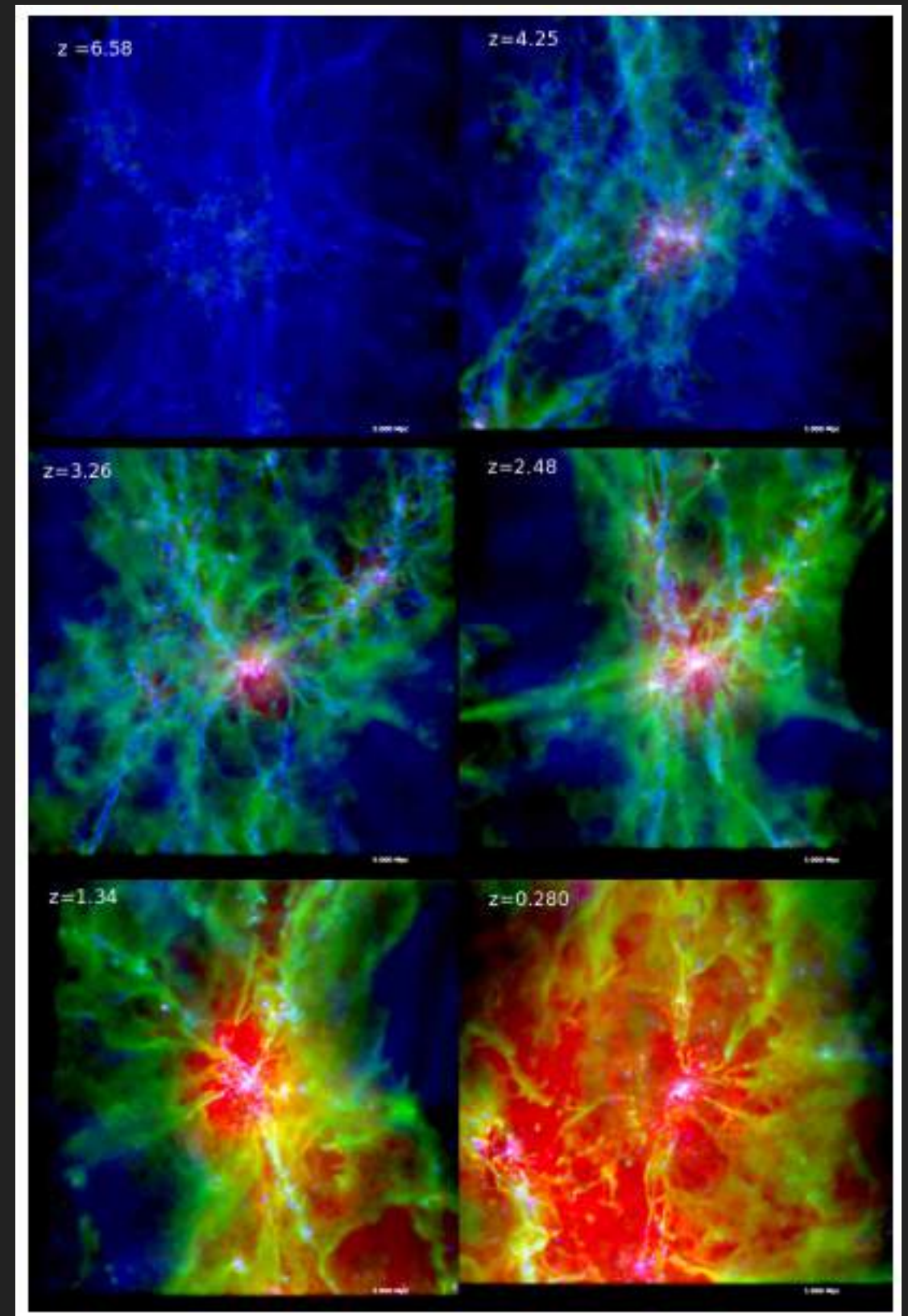
AGN feedback models in cosmological simulations assume that the accretion rate on the blackhole based on the Bondi-Hoyle-Lyttleton formula.

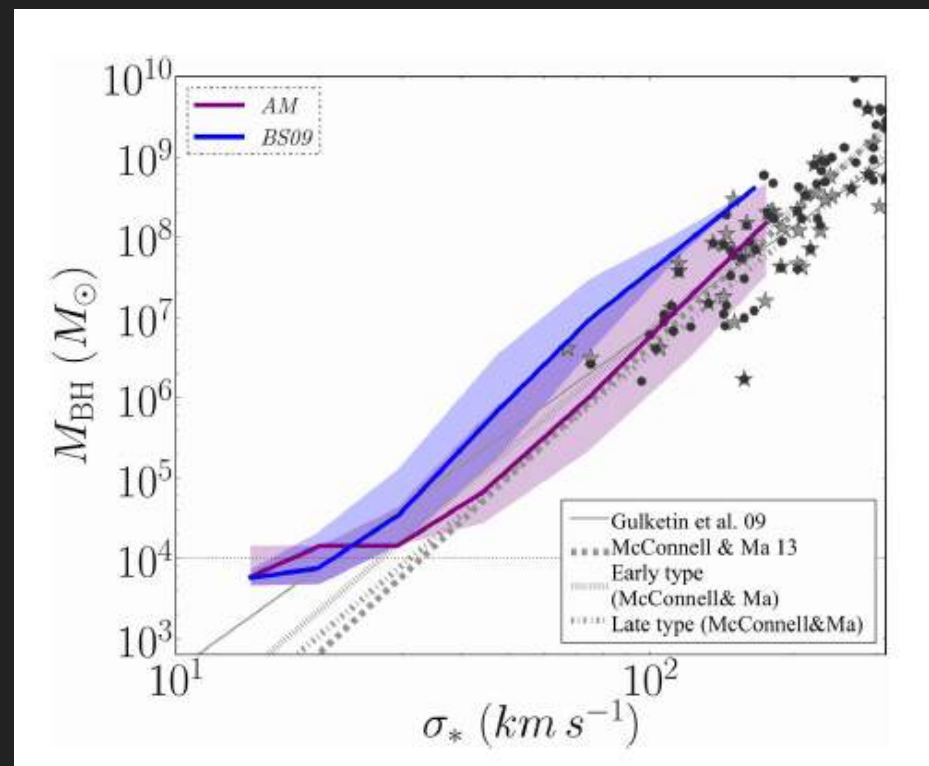
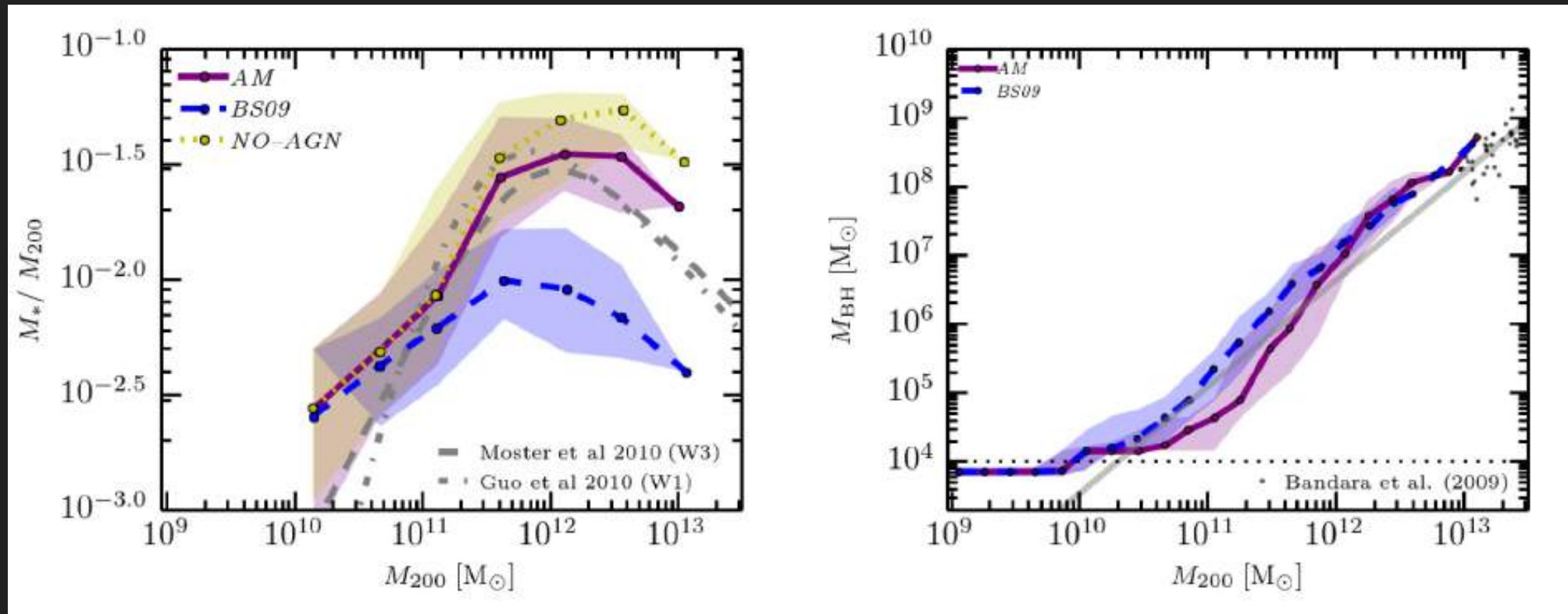
$$\frac{dM_{\text{BH}}}{dt} = \alpha_{\text{boost}} \frac{4\pi G^2 M_{\text{BH}}^2 \rho}{(c_s^2 + v_{\text{rel}}^2)^{3/2}}$$

In general, these models reproduce the galaxy and black hole masses (Di Matteo 2005) at the high mass end, The evolution of the BH population and agn luminosity across cosmic time.

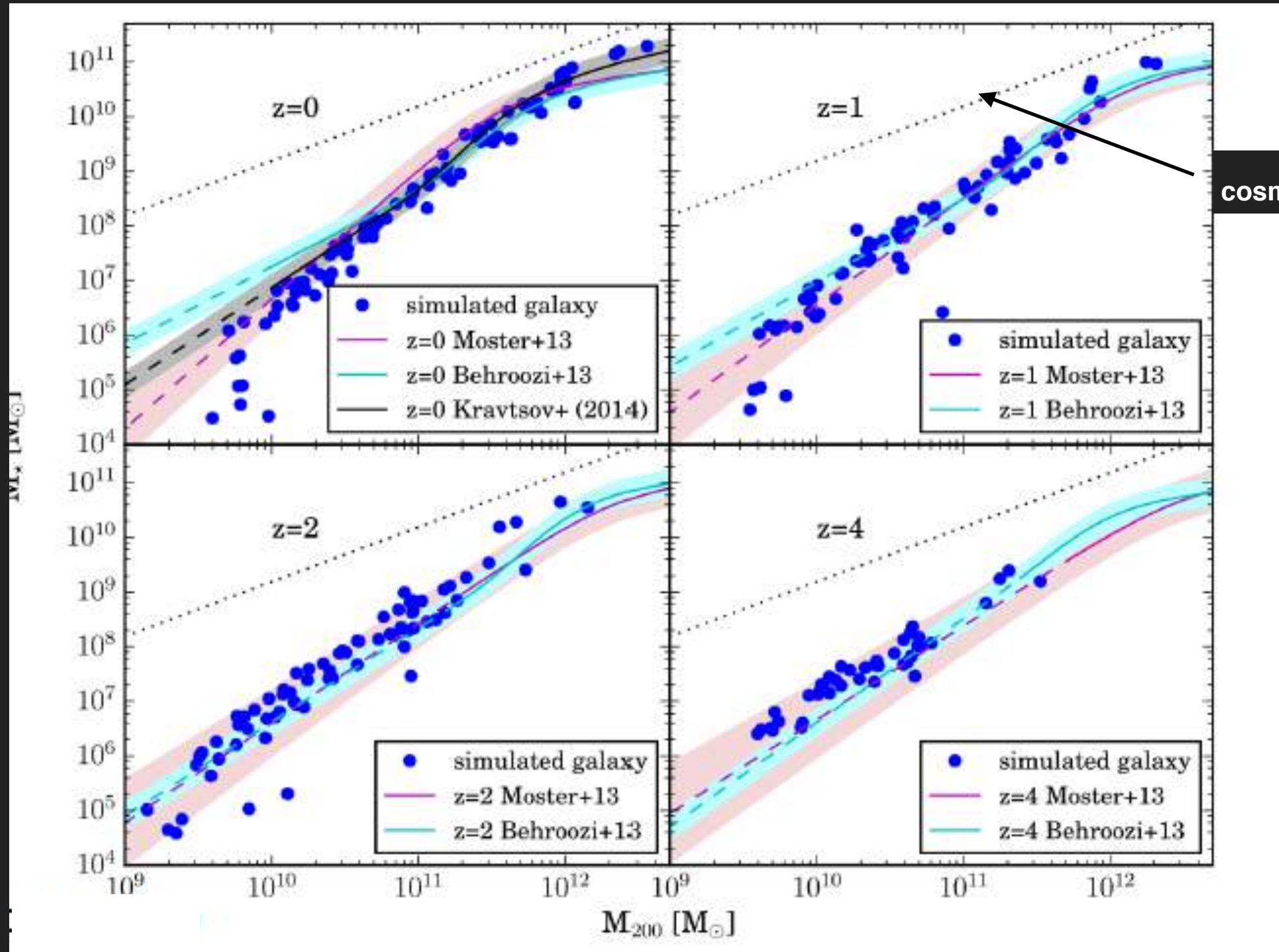
Several approaches have been developed in different numerical codes (e.g. Springel+2005; Dubois+2012; Rosa-Guevara+2015; Sijacki+2015; Hopkins+2016; Springel+2016)

Different response depending on the halo mass



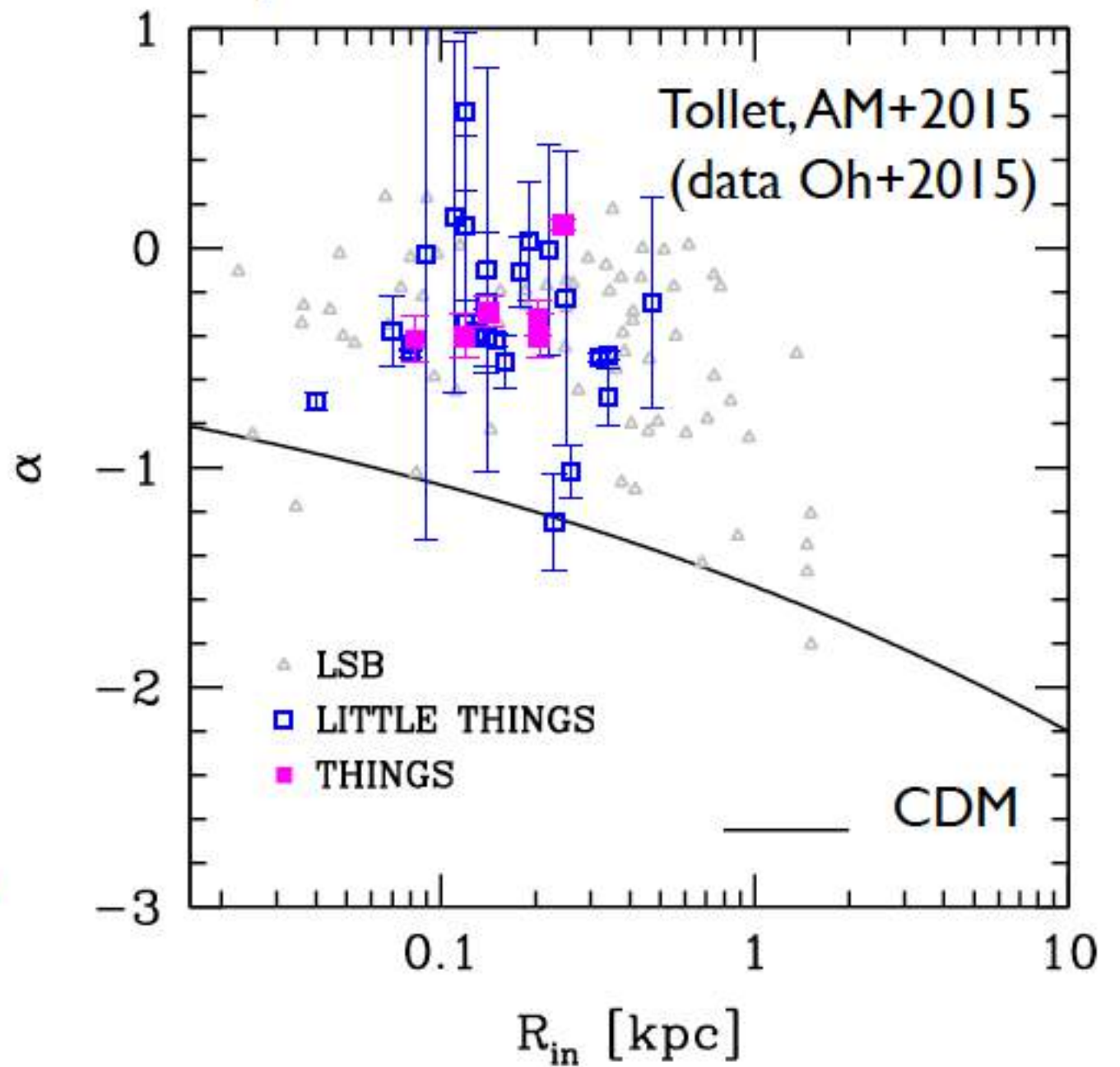
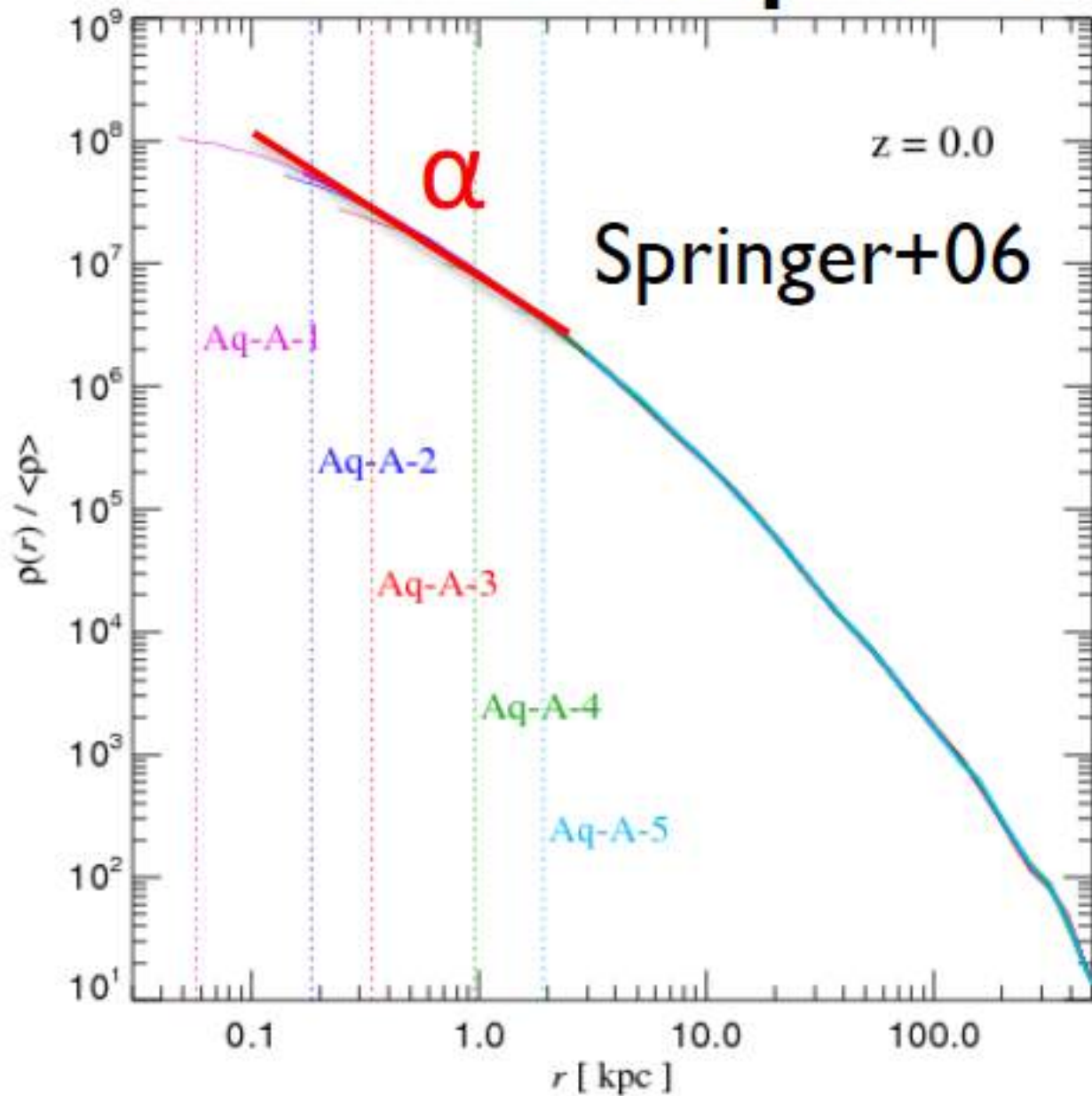


AGN feedback models can be tuned to reproduce the MBH- σ star relation and the $M_{\text{star}}/M_{\text{halo}}$

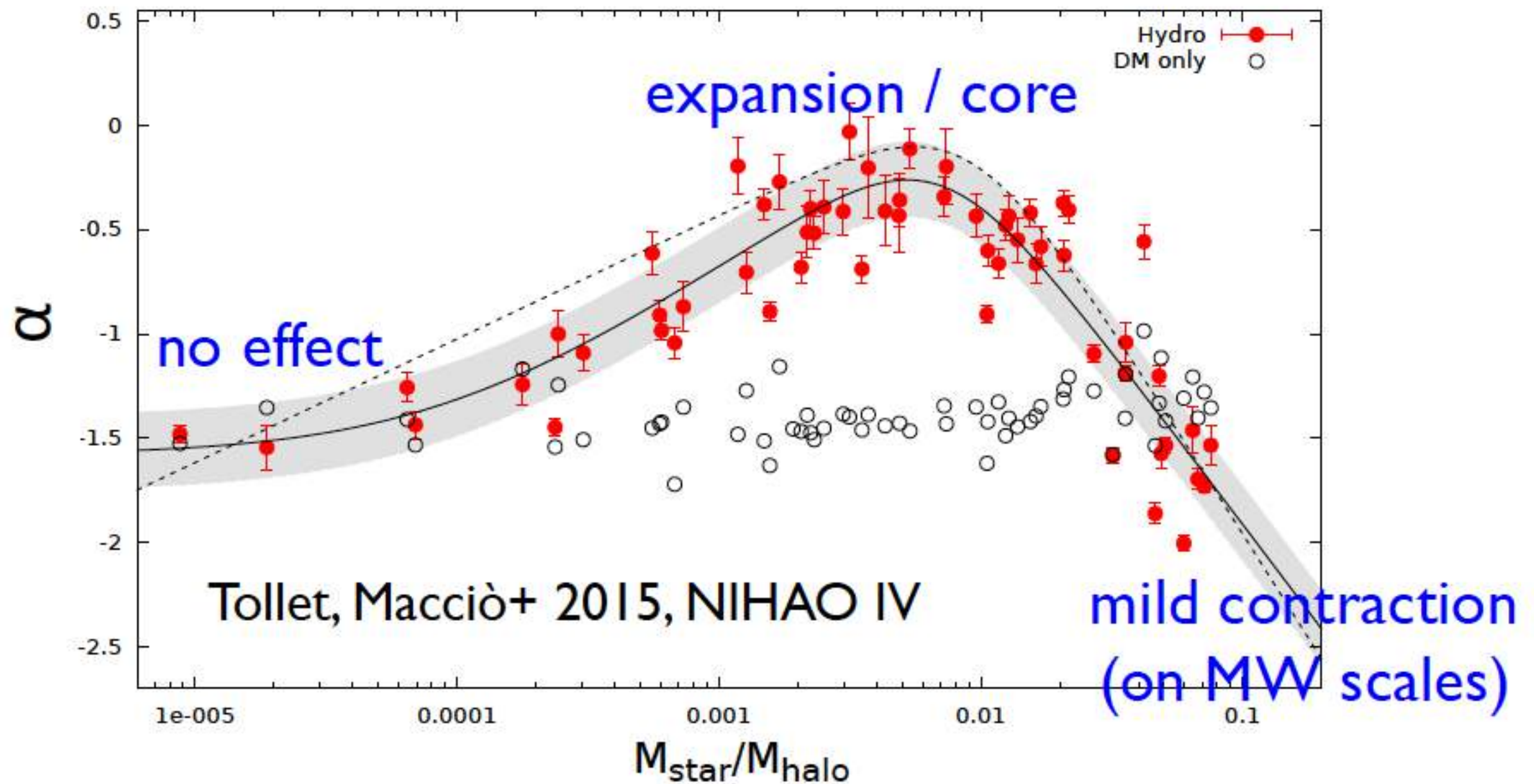


**NIHAO project:
Evolution of the $M_{\text{star}}/M_{\text{halo}}$**

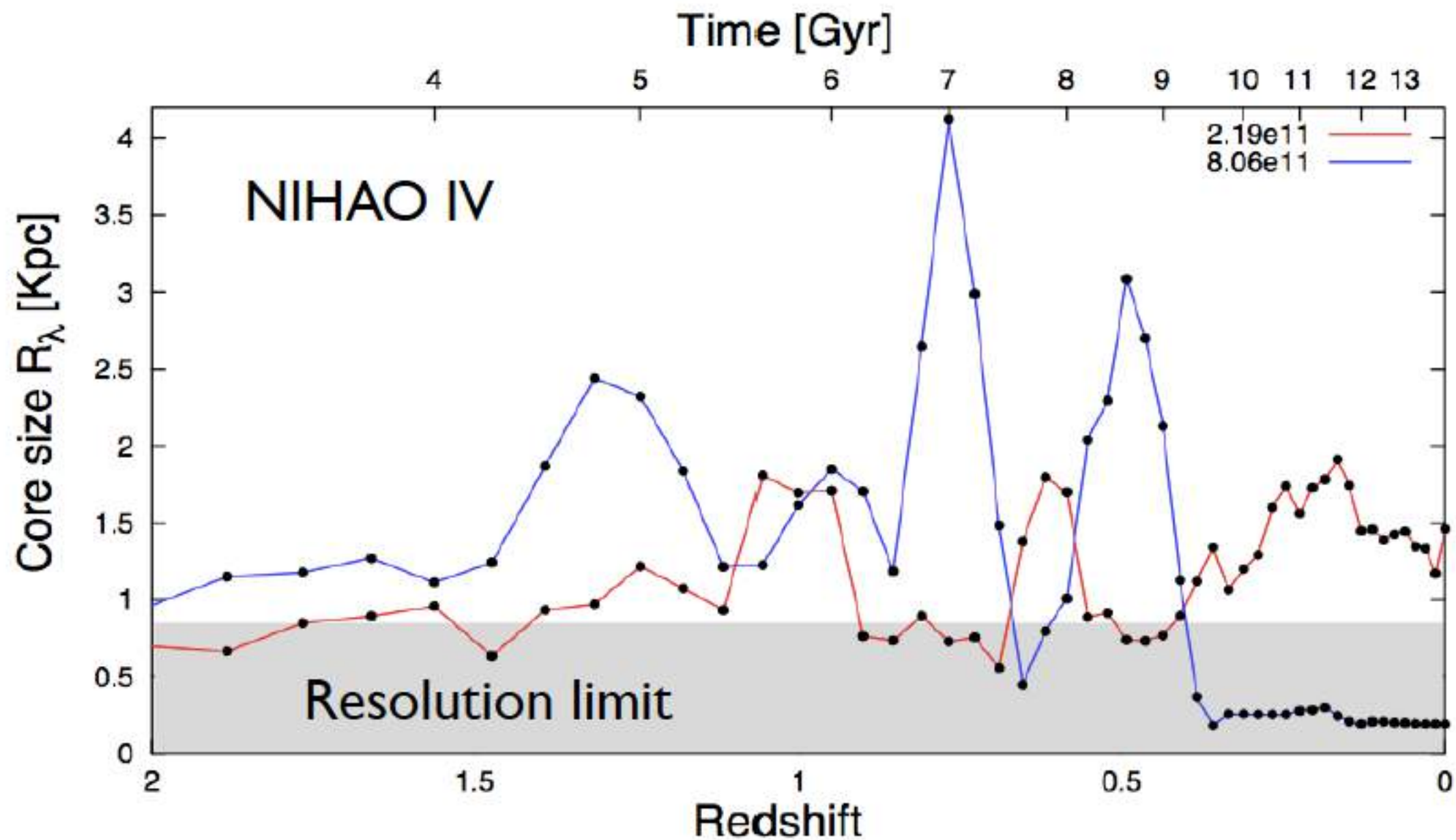
Cusp vs. core problem



The DM distribution in NIHAO



Core creation and core destruction



courtesy of A. Maccio

Is this the core/cusp problem solve?